HEAT EFFECTS IN ADSORPTION: MODELING WITH EQUATIONS OF STATE FOR CONFINED FLUIDS

A Thesis

by

SHADEN MOHAMMED HASSAN DAGHASH

Submitted to the Office of Graduate and Professional Studies of
Texas A&M University
in partial fulfillment of the requirements for the degree of

MASTER OF SCIENCE

Chair of Committee,	Marcelo Castier
Committee Members,	Ibrahim Galal
	Ioannis Economou
	Shaheen Al Muhtaseb
Head of Department,	M. Nazmul Karim

May 2016

Major Subject: Chemical Engineering

ABSTRACT

Adsorption is valuable for industrial separation and purification processes and the characterization of porous materials. The amount of adsorbate a given adsorbent can take at a given condition and the associated heat effect are among the most important data for adsorption phenomena. In particular, the study of heats of adsorption plays an important role in the assessment and optimization of energy use in industrial processes. That is because the adsorption process temperature is a key factor that controls local adsorption equilibria and dynamics within adsorption columns. There are different definitions and experimental measurement techniques of heats of adsorption, but this work's focus is on predicting isosteric and pseudo-isosteric heats of adsorption and the difference in specific heat capacity between the adsorbed and the bulk phases of a gas on an adsorbent using an equation of state for confined fluids. The equation of state used extends the Peng-Robinson equation of state for fluids within solid spherical pores. The adsorption of a variety of pure gases on different zeolites is studied in this research. Zeolites of types A and X are the main focus as they are the adsorbents utilized in many gas adsorption-separation processes. Adsorption isotherms are correlated by means of parameter fitting and their average absolute relative deviations (AARDs) are in the range 1% – 6% for most of the studied systems. The results of isosteric and pseudo-isosteric heats of adsorption are predictions, which generally follow the qualitative experimental trends and have AARDs in the range 21% - 46%. The calculated isosteric heats were

used to reflect on the zeolite heterogeneity and energetic levels and to calculate the difference in specific heat capacities. This was in the range of -0.5R to 3R, which is the same order of magnitude of results obtained from literature.

ACKNOWLEDGEMENTS

I would like to acknowledge my committee chair, Prof. Marcelo Castier, and Prof. Shaheen Al Muhtaseb for their outstanding technical assistance, effectively co-supervising this work. In addition, I thank my committee members, Prof. Ibrahim Galal and Prof. Ioannis Economou for their supervision and great support throughout the period of this research. I would like also to thank Prof. Vassilios Kelessidis for his support.

Many thanks go to my friends and colleagues and the department faculty and staff for making the time I spent at Texas A&M University at Qatar a magnificent experience and a fruitful journey for me. Finally, all the thanks go to my mother, father, brothers, and sister for their encouragement and special thanks for my husband and children for their patience, support, and love.

NOMENCLATURE

a_p	Confinement-modified energy parameter of the fluid mixture
b_p	Confinement modified volume parameter
$c_{p,a}$	Adsorbed phase specific heat capacity
$c_{p,g}$	Gas phase specific heat capacity
Δc_n	The difference is specific heat capacity
F_{pa}	Fraction of confined molecules in the square-well region
h_s	Molar enthalpy of the fluid in the adsorbed phase
h_g^o	Molar enthalpy of the fluid in the ideal gas state
h_g	Molar enthalpy of the adsorbate in the gas phase
$\bar{H}_g$	Partial molar enthalpy of the adsorbate in the gas phase
$\bar{H}_a$	Partial molar enthalpy of the adsorbate in the adsorbed phase
h^a	Molar enthalpy of the fluid in the adsorbed phase
h^b	Molar enthalpy of the fluid in the bulk phase
H^e	Excess enthalpy of the fluid in the confined (adsorbed) phase
Δh_s	Enthalpy change on adsorption
$-\Delta h_s$	Isosteric heat of adsorption
k_{ij}	Binary interaction parameter
M	Cation that occupies the sites of the zeolite
M_s	Mass of adsorbent
N	Valence of cation M

N_{av}	Avogadro's number
n	Loading/adsorbed amount
n_{ac} and n_{ae}	Correlated and experimental adsorbed amounts
P_a and P_b	Pressures of the adsorbed and bulk phases
∂Q	Differential change in energy
q_{iso}	Isosteric heats of adsorption
$q_{p\text{-}iso}$	Pseudo-isosteric heats of adsorption
R	Universal gas constant
r	Pore radius
S	System entropy
T	System temperature
U	System internal energy
X	Component mole fraction in bulk phase
x, y	Integers in zeolite formula
Z	Number of water molecules in each unit cell in zeolite formula

Greek Letters

δ_p	Square well width of the molecule-wall interaction potential
ε_p	Square well depth of the molecule-wall interaction potential
θ	Geometric factor of the model
μ_s, μ_g	Chemical potential of component in the adsorbed and gas phases
μ_g^o	Standard chemical potential of the gas phase

v	Fluid molar volume
v^b	Bulk phase molar volume
v^a	Adsorbed phase molar volume
σ	Molecular diameter
$\emptyset_a$ and $\emptyset_b$	Fugacity coefficients of the adsorbed and bulk phases
ω	Acentric factor

TABLE OF CONTENTS

Page

LIST OF FIGURES

Page

LIST OF TABLES

Page

CHAPTER I

INTRODUCTION-RESEARCH PROBLEM AND OBJECTIVES

Modeling of fluid adsorption is critical to the design and optimization of efficient adsorption-based separation and purification processes. A key effect is that properties of confined fluid inside the pores of an adsorbent differ significantly from those of the bulk fluid. The difference is attributed to the geometric constraints that confinement imposes on the fluid molecules and to the interactions of fluid molecules with adsorbent pore walls [1]. Gas adsorption isotherms, heats of adsorption, and adsorbed phase heat capacity are key factors in the design and development of adsorption processes because they affect their mass and energy balance calculations. The energy balance of the adsorption process identifies the amount of heat released during adsorption processes and the needed heating for desorption (regeneration) processes.

Despite the amount and variety of research done on heats of adsorption, there has not been an agreement by researchers on a unified definition of its meaning. This research aims to explore the different available definitions of heats of adsorption as to understand their physical meaning. This is needed to serve the main goal of this research, which is to check the ability of an existing thermodynamic model in predicting heats of adsorption. The model accounts for confinement effects, which are highly pronounced specially for small pore-sized adsorbents. The importance of such model comes from the fact that some types of heats of adsorption - such as isosteric heats - are

difficult to be measured experimentally; thus the availability of a good model to predict them is of great significance to the optimization of adsorption processes.

There are two main challenges of this research project. The first one is a theoretical challenge that involves understanding and analyzing the several definitions of heats of adsorption available in literature and connect them to the work done in this research and the conducted derivations and equations used to estimate heats of adsorption. This is extremely imperative as it will be reflected on the quality of predictions of these heats done by the model proposed in this work. The other challenge is a practical one, which involves testing the model for its ability to correlate adsorption isotherms at different ranges of temperature and pressure and in validating the model's capability to accurately predict heats of adsorption from residual properties as well as estimating the adsorbed phase heat capacity from predicted heats of adsorption.

The equation of state proposed in this research is considered to be of intermediate complexity compared to simple isotherms and molecular simulation methods currently available. The model works with the main assumption that the interactions between the molecules of the fluid and the pore wall follow the square-well potential. In this model, the pore size is represented by a pore diameter, and the nature of the fluid – pore wall interactions is taken into consideration. The interactions between fluid and pore walls as well as the interactions between fluid molecules inside the pores are considered (which are often neglected in some current models). The model used in this work is based on the generalized van der Waals theory and extends the Peng-Robinson equation of state. It has the advantage of making it possible to use the same equation of state for all phases

(bulk and confined) so that the existing procedures for phase equilibrium calculations can be refitted to perform equilibrium calculations for confined fluids.

This model for confined fluids can be used to simulate conditions for adsorption equilibrium in heterogeneous solids accounting for different pore sizes of the adsorbent and different interactions with the fluid. In this work, it is tested by using it to evaluate and analyze adsorption properties (adsorption isotherms, heats of adsorption, and adsorbed phase heat capacity).

In this thesis, a deep and thoughtful literature review was conducted on gas adsorption with focus on adsorption isotherms, heats of adsorption, and adsorbed phase heat capacity to identify the main outcomes of other researchers' work on the same area and reflect on how they define these heats and what models they developed to predict them. The first tasks that were done, were the collection of experimental adsorption equilibrium data and calorimetric measurements of heats of adsorption for the specific systems studied in this work. The calculation part which is the heart of this thesis involves three different stages of calculations. The first one is the adsorption isotherms correlations which is critical in order to test and validate the model's capability to fit experimental adsorption isotherms. The second stage is the calculations of heats of adsorption of a collection of pure gases on selected zeolites and comparing the obtained results with calorimetric measurements found in different references, as well as comparing them to the heats calculated using the Clausius – Clapeyron equation or other model results available. The third and final stage of the calculations conducted in this thesis is the estimation of the adsorbed phase heat capacity using the isosteric heats of

adsorption predicted by the model and the reflection made on the obtained order of magnitude in comparison with literature findings. A thorough discussion of the results of calculations described above as well as main concluding points and highlights of future work that can be done to improve the performance of the model follow the presented results.

CHAPTER II

LITERATURE REVIEW

2.1. Introduction to gas-solid adsorption

The adsorption phenomenon was first recognized when it was noticed that the concentration of molecules of a gas phase increased near a solid surface [2], [3]. Later, the term “adsorption” was used to describe this phenomenon. The adsorption phenomenon has a great value as it is globally used in industry for gas separation and refining processes and because of its important role in determining the characteristic of porous materials. The study of gas adsorption on solid surfaces reveals information on the volume and size of micropores, the area of mesopores, and heats of adsorption [2].

The meaning of adsorption can be understood by noting that the bonds of a clean solid surface are not all saturated, which causes an “adsorption field” to exist on the surface. Due to this “adsorption field”, molecules of a fluid accumulate near the surface [2]. However, the big share of adsorption process happens inside the pores of the solid, which are characterized by great surface area per unit mass of solid (using highly porous solid particles with micropores). Depending on the concentration of the feed, adsorption can be categorized as a “purification” or “bulk separation” process [4]. When gas adsorption occurs, the system consists of: (i) bulk phase (or the free gas phase of molecules that are not adsorbed and surrounds the solid surface), and (ii) the adsorbed phase (or confined phase of adsorbed molecules on the adsorbent surface and inside its pores). Adsorption is a process that is identified by adsorption isotherms, heats of

adsorption, adsorption kinetics, and surface thermodynamic properties of energy and entropy [5].

Depending on the type of the interactions between the adsorbate and the adsorbent, adsorption can be classified into two major categories:

(i) Chemisorption, in which chemical bonds between the gas molecules and the surface of the solid are formed [6].

(ii) Physical adsorption, which involves two types of weak bonding: (a) van der Waals forces that are always present in adsorption and (b) electrostatic forces (also called coulombic forces) that are substantial only when specific types of adsorbents with ionic structure - such as zeolites - are used [3].

In physical adsorption (also known as "physisorption"), the electrostatic bonds are much weaker than van der Waals interactions, which makes it an easily reversed process [6]. Physical adsorption takes place primarily inside the adsorbent pores and at its external surface.

Almost all adsorption-based separation processes depend on physisorption rather than on chemisorption. Physisorption has relatively low heats of adsorption compared to chemisorption, and it happens mostly at relatively low temperatures. Adsorbed molecules do not dissociate or change their molecular structure and can be adsorbed in one layer or multilayers. Physical adsorption is rapid, non-activated, and reversible process that does not experience the transfer or share of electrons between the adsorbate and the adsorbent nor among the adsorbate molecules, although polarization of adsorbate molecules can take place [3]. For a system of constant temperature and volume, the

amount of adsorbed gas in a confined space can be determined by monitoring the system pressure. A decrease in the system pressure indicates that adsorption of gas is taking place.

A typical adsorption system consists of an adsorptive gas, a sorbed phase or adsorbate that includes the gas components with concentrations different than in the bulk (gas) phase. There is a difference in concentration between the gas and the adsorbed phases that is basically due to the different interactions the two components have with the solid sorbent or adsorbent atoms. The adsorption process happens when the transfer of molecules from the fluid phase to the surface of the solid phase takes place. It is an exothermic process that involves the release of heat, unlike desorption which is the transfer of molecules from the solid adsorbent surface to the fluid phase and is an endothermic process [7].

Compared to a "distillation" unit, a gas adsorption unit with the same number of theoretical stages has higher cost, but at the same time, much higher separation factors are attained in it. For systems with "relative volatility" less than 1.25, distillation is considered incompetent and adsorption is much more cost-effective if a suitable adsorbent exists. This is specifically observed in important industrial processes that involve the separation of mixtures into several streams, each enriched with a valuable pure product. In case of streams with very close boiling point components, an adsorption unit with proper type of adsorbent, is more economical and energy-saving than distillation [3].

A successful adsorption process depends on many factors, one of which is the selection of the suitable solid material to be used as an adsorbent. There are specific characteristics for an adsorbent to be considered suitable for commercial applications. A suitable adsorbent must be of low cost and have high selectivity to specific components. It should also be of high capacity to minimize the amount used. In addition to that, it should be stable (chemically and thermally), hard and mechanically strong to avoid crushing and erosion. A good adsorbent should also have high resistance to fouling, no tendency to promote undesirable chemical reactions, and to have free-flowing tendency to be easily filled/emptied from vessels [4]. More details about the available different types of adsorbents will follow in next sections.

When approaching adsorption in general, a discussion on confinement effects has to be clearly highlighted. When fluid is adsorbed on a porous solid, adsorption happens mainly inside the pores of the solid as well as its surface. Here, the thermodynamic behavior of confined fluids inside the pores is a subject of ultimate significance for further studies and inspection due to its major impact on the performance of adsorption processes in industrial applications. Some of these applications involve separation, extraction, and catalysis. The importance of the thermodynamics and equilibrium phase behavior of confined fluids arises from the fact that they are indispensable for the design and optimization of separation processes [1].

Fluid behavior in the confined phase differs from its behavior in the bulk phase due to the geometrical limitation that the fluid molecules have as well as their interaction with the pore walls (or basically the molecule–wall interactions). The change of fluid

properties under confinement has been investigated over the years by many researchers theoretically and by molecular simulation, aiming to develop thermodynamic relations that can be used to predict confined fluid behaviors [1].

2.2. Thermodynamics and equilibrium of gas-solid adsorption

In 1984, Ruthven [3] described adsorption equilibrium to be a form of general phase equilibrium with an inherent assumption that the adsorbed layer can be treated as a distinct phase. This is an acceptable assumption, despite that the adsorption phase boundary location is not really known [3]. The basics about adsorption thermodynamics and equilibrium were revealed by the work of Hill, Everett, Young, and Crowell over the past years [3].

The concept behind applying the basics of classical thermodynamics to adsorption involves considering that the surface layer, which consists of adsorbent and adsorbate as a single phase, has the main properties of a solution. According to Ruthven, if the geometric properties and the thermodynamics of the adsorbent can be considered independent of the surrounding gas temperature and pressure, then the adsorbent can be considered as “thermodynamically inert”. In this case, the adsorbed molecules can be considered as a distinct phase and the only effect the adsorbent has on them is the creation of adsorption force field [3].

As most of adsorption-based separation processes depend on physical adsorption, its thermodynamics is further discussed in this section. Physical adsorption has been the focus of much research as it has many applications on industrial scale. Understanding

the thermodynamics of physical adsorption is the key to develop new models that can describe the behavior of different adsorption systems, which may lead to enhanced overall design and energy saving in adsorption units of large scale.

Gas - solid adsorption equilibrium is usually expressed in terms of adsorbate loading or the amount of adsorbate that is adsorbed on the solid. This amount can be in units of mass, mole, or volume of adsorbate per unit surface area (or mass) of the adsorbent [4]. According to Ruthven, in the case of a uniform surface of low adsorbate coverage, the fluid phase and the adsorbed phase concentration have a linear equilibrium relation that is known as Henry's law. A low concentration in this case is defined as a concentration low enough to make all adsorbed molecules isolated from each other. Henry's law specifies that, at constant temperature, the amount adsorbed increases as the partial pressure of the species in the gas phase - in equilibrium with the liquid - increases. The application of Henry's law helps in screening adsorbents for specific adsorption processes. When adsorption equilibrium is reached in a system, the chemical potential of each adsorbed species in all phases (adsorbed and bulk) should be equal [3].

As Myers [8] explained in his work, enthalpy, entropy, and Gibbs free energy are used to describe the thermodynamics of the adsorption system as they are used in essential applications such as the characteristics of the adsorbent, adsorption of pure components and mixture, molecular simulation, enthalpy balances, calorimetric properties, and shape selectivity in catalysis [8].

In order to understand the thermodynamics and equilibrium in adsorption processes, scientists and researchers have been conducting different studies and have

tried to model the "confined fluid" in pores of the adsorbent. Confined fluids have properties that differ from the bulk phase properties due to the effect of confinement that increases the interactions among gas molecules themselves as well as the interactions between gas molecules and walls of the pore. Confinement effects are inversely proportional to the pore size, i.e., they increase as pore diameter decreases.

Travalloni *et al.* [9] focused on modeling the confined fluid inside adsorbent pores using equations of state. Their work highlighted the importance of estimating and predicting confinement effects on species adsorbed inside the pores based on pore size, shape, and characteristic energy. This is very critical in variety of processes such as separation and oil reservoirs in which the heterogeneity of the adsorbent is a key factor. Most of the current models do not account for as many confinement details and are limited to the adsorbent surface heterogeneity, which limits the knowledge about adsorption in adsorbents with wide size pore distribution [9].

Properties of confined fluids are often estimated using molecular simulation or density functional theory. Both methods require long computations [9]. Due to this, this work focuses on models that can be used to predict confined fluid properties in less details, yet with enough precision for engineering design. However, it must be recognized that for a detailed representation of confined fluid properties that accounts for both microscopic and macroscopic behaviors, molecular simulation is a must.

2.3. Adsorption isotherms

Adsorption isotherms are plots of loading (amount adsorbed) of the adsorbate versus the system bulk pressure at a certain (constant) system temperature. They are obtained by collecting experimental data using the volumetric or gravimetric methods. Adsorption isotherms are needed for the design of adsorption-separation systems. There are five types of physical adsorption isotherms that a system can follow as shown in Figure 1. This classification was given by Brunauer [10] who named them as van der Waal adsorption isotherms [10]. These were discussed by Ruthven [3] in his work and are presented in Figure 1.

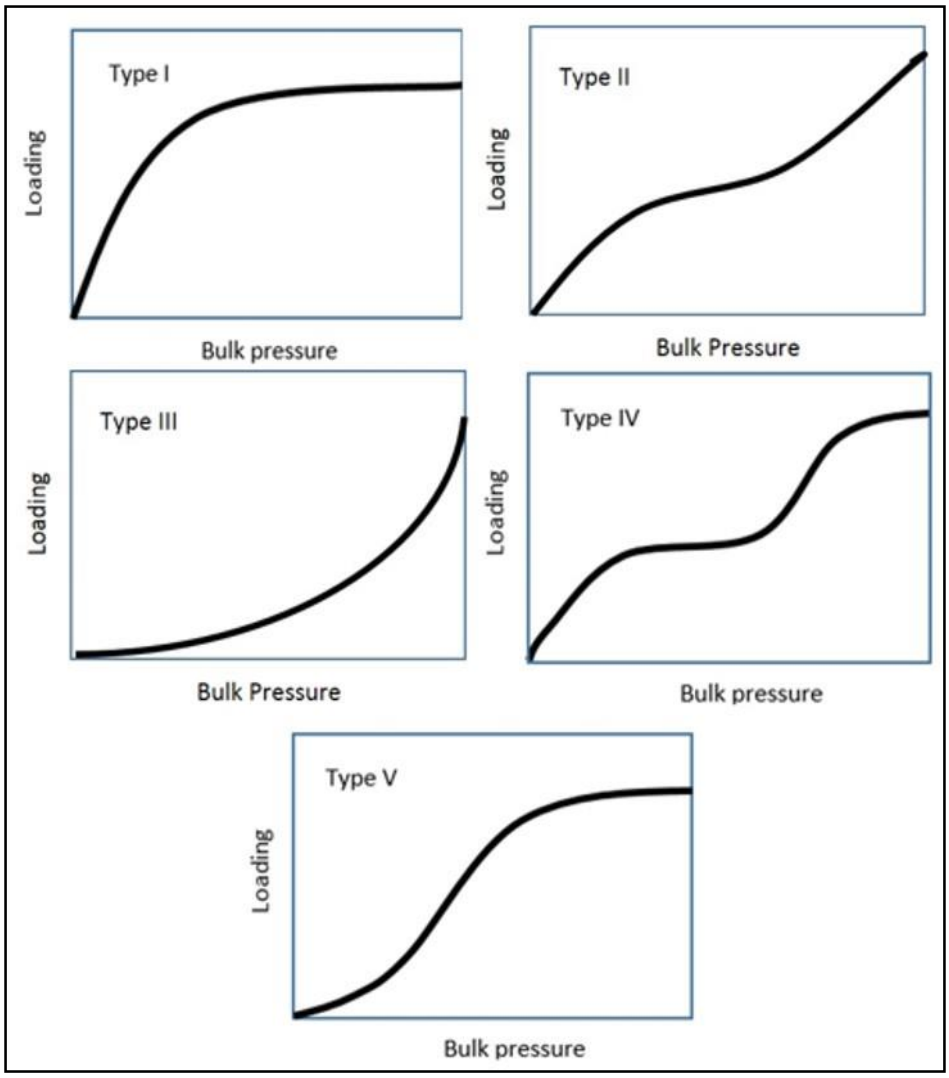

Figure 1: Brunauer's five adsorption isotherms (adapted from [3])

Type-I isotherm is usually associated with adsorption on microporous adsorbents in which the pores are of almost the same size as the diameter of the adsorbate molecule. This is due to the fact that with this type of adsorbents there is a certain saturation limit for the complete filling of the micropores [3]. Type-I is associated with strong

adsorption. This type is what defines monolayer adsorption and it is observed in adsorption of gases at temperatures that are above their critical points [4].

Type-II isotherm can be observed with adsorbents of wide range of pore sizes [3]. This type experiences strong adsorption, but it is usually a characteristic of multilayer adsorption of the BET type. This type is applicable to adsorption of gases at temperatures that are below (but approaching) their critical points. For this type, the heats of adsorption (to be discussed later) of the first adsorbed layer is greater than that of the succeeding layers as these layers are assumed to have heat of adsorption that is the same as the condensation heats [4]. Types I and II are usually observed in adsorption separation processes [6].

Type-III isotherm is also observed in adsorbents that have wide ranges of pore size distributions [3]. It is associated with small extent of adsorption at high pressures. It is also a characteristic of multilayer adsorption. The heat of adsorption of the first layer is the lowest compared to that of the following layers, and this isotherm is rarely observed [4].

Type-IV isotherm is associated with adsorption in which two adsorbed layers are formed on the adsorbent surface or inside the pore of size that is much larger than the diameter of the adsorbate molecule [3]. Type-IV isotherm is considered as the capillary condensation version of type II [4].

Type-V isotherm is observed when adsorbate intermolecular attraction effects are large [3]. Type V isotherm is also considered as the capillary condensation version of type III [4]. For adsorbents with wide range of pore size, an incessant increase with

increasing adsorbed amount takes place as adsorption goes from monolayer to multilayer until it reaches finally capillary condensation. The increase in adsorbed amounts at high system pressures is due to capillary condensation that takes place inside pores of larger diameter while the pressure is elevated [3].

According to Yang [6], three methods can represent isotherm model. The first of them is Langmuir method, which was developed in 1918. The main assumption of this method is that the system under adsorption is in dynamic equilibrium. It assumes that both of the adsorption and desorption rates are equal. The second is Gibbs method that employs the Gibbs adsorption isotherm. This method assumes that the adsorbed film is presented using a two dimensional equation of state. The third is the potential method which was developed in 1914. In this method, the adsorption process is presented by a gradual concentration increase of gas molecules as they approach the solid surface because of the potential field at the surface [6].

2.4. Heats of adsorption

Heat of adsorption is an important topic in the field of adsorption and has been the subject of many publications and books. It is a key factor in the study and optimization of energy use in adsorption processes. An early discussion of heats of adsorption was made by Hill [11] in 1949. As he pointed out, the actual definition of the type of calorimetric heats usually measured is ambiguous. Different researchers use different apparatuses and experimental procedures in order to measure them. However, different methods give different types of heat of adsorption [11].

As there are many experimental and theoretical studies on the thermodynamics and equilibrium of gas adsorption in porous solids, there are multiple definitions of heats of adsorption. A general definition by Valenzuela and Myers [12] states that heats of adsorption are the difference between the energy of the adsorbate in the bulk phase and in the adsorbed phase. They refer to four categories of heats of adsorption: the isosteric heat (which is considered in flow systems), the differential heat (which is considered in batch systems), the integral heat (which is considered for batch systems as well), and the equilibrium heat (which reflects the molar change of the enthalpy of the adsorbate) [12].

Differential heats - which are also referred to as difference in partial molar energy - are defined as a calorimetric measurement that is carried out at constant volume [3]. It is also defined as the difference between isosteric heat of adsorption and the product of the universal gas constant and temperature, RT [8].

Equilibrium heats of adsorption can be obtained by differentiating the isosteric heats of adsorption at constant spreading pressure [8]. This makes this type of heat difficult to be obtained experimentally due to the difficulty in measuring and calculating spreading pressure inside the micro-pores [13].

The isosteric heat of adsorption is the focus of this work as it is usually used in the study of heat effects and energy balance on adsorbers, such as the work done by Walton and Levan [14] in developing energy balance equations for fixed-bed adsorption columns. Some definitions of this type of heats are presented in this section.

Myers [8] has defined isosteric heats of adsorption with the following equation:

$$q_{iso} = RT^2 \left[\frac{\partial lnP}{\partial T}\right]_n \qquad (2.1)$$

where P is the system pressure and n is the adsorbate loading or amount adsorbed.

As Myers discussed in his work, the isosteric heat of adsorption are found by the differentiation of a group of adsorption isotherms at constant loading n. Equation (2.1) can be applied to pure gases assuming that they behave as ideal gas [5], [8] and that the volume of the adsorbed phase is negligibly small in comparison with the volume of the bulk phase [5]. The same reference defines the isosteric heats of adsorption as the differential change in energy that is released when an inconsiderable amount of the adsorbate is transferred from the bulk phase to the adsorbed phase at constant pressure, temperature, and adsorbent mass. This is similar to the definition presented by Ruthven and discussed in details below. Their definition of isosteric heats Q_{st} is presented in equation (2.2):

$$q_{iso} = \left[\frac{\partial Q}{\partial n}\right]_{T,P,M_s} \qquad (2.2)$$

where ∂Q is the differential change in energy and M_s is the mass of adsorbent [5]. Based on this definition, the authors developed a procedure to predict the isosteric heats of adsorption, which is based on the implicit, yet unrealistic, assumption that the pressures in the bulk and adsorbed phases are equal. Their formula is presented in equation (2.3). Where m_a and m_g are the molecules masses in adsorbed and gas phases, respectively and v^b is the bulk phase molar volume. The first part of the equation is the Clausius Clapeyron equation, and the second part accounts for the non-ideality of the gas phase.

$$q_{iso} = RT^2 \left(\frac{\partial lnP}{\partial T}\right)_{m_a} + Tv^b \left(\frac{\partial P}{\partial T}\right)_{m_g} \qquad (2.3)$$

Karavias and Myers [15] define the isosteric enthalpy of adsorption as the difference between the molar enthalpy of the fluid in the bulk phase and the excess molar enthalpy of the fluid in the adsorbed phase [15]:

$$q_{iso} = h^b - h^e \tag{2.4}$$

where:

- h^b: molar enthalpy of fluid in the bulk phase.
- h^e: excess molar enthalpy of fluid in the adsorbed phase.

Ruthven [3] defines isosteric heats as the heat transferred to the surroundings when the transfer of a differential quantity of adsorbate from the vapor phase to the adsorbed phase takes place under isothermal and isobaric conditions [3]. Ruthven's derivations of isosteric heats of adsorption start with the adsorption equilibrium condition where the main assumptions are that the chemical potential of all adsorbed species in all phases is equal and that the bulk phase behaves as an ideal gas:

$$\mu_s = \mu_g \tag{2.5}$$

$$\mu_s = \mu_g = \mu_g^o + RT\ln\left[\frac{P}{P_o}\right] \tag{2.6}$$

where $\mu_s \; and \; \mu_g$ are the chemical potential of adsorbed and gaseous phases respectively and μ_g^o is the standard chemical potential of the gas phase at the reference pressure P_o. Using the Gibbs – Helmholtz relation given by:

$$\frac{\partial\left(\frac{\mu}{T}\right)}{\partial T} = -\frac{h}{T^2} \tag{2.7}$$

Differentiating equation (2.6) at constant adsorbed phase concentration (q, mol/volume) and applying the Gibbs – Helmholtz relation, the obtained equations are:

$$\frac{-h_s}{T^2} = \frac{-h_g^o}{T^2} + R\left(\frac{\partial lnP}{\partial T}\right)_q \quad (2.8)$$

$$\left(\frac{\partial lnP}{\partial T}\right)_q = \frac{h_g^o - h_s}{RT^2} = \frac{h_g - h_s}{RT^2} = \frac{-\Delta h_s}{RT^2} \quad (2.9)$$

Now, the following can be defined:

- Enthalpy change on adsorption: $\Delta h_s = h_s - h_g$ (2.10)
- Isosteric heat of adsorption: $-\Delta h_s = h_g - h_s$ (2.11)

where h_s is the molar enthalpy of the adsorbed phase and h_g^o is the molar enthalpy of the ideal gas. Integration of equation (2.9) under these conditions results in:

$$\ln P = \text{constant} - \frac{\Delta h_s}{RT} \quad (2.12)$$

Isosteric heats of adsorption can be obtained in a simple and feasible way by plotting (lnP) versus (1/T) which will give a linear isostere with the slope ($-\Delta h_s/T$) [3].

Similar to the analysis done by Myers [8] and Ruthven [3] is the work done by Sandler *et al.* [16]. They defined isosteric heats of adsorption as the change in enthalpy obtained from adsorption isotherms at constant loading at multiple temperatures. They differentiated equation (2.5) with respect to temperature at constant loading to get the partial molar enthalpy of an adsorbed species. It is important to realize that the partial molar enthalpy of an adsorbate in adsorbed phase is not equal to the partial molar enthalpy of an adsorbate in the bulk phase and this is due to the fact that the derivative is taken at a constant number of moles of the adsorbed phase [16]. The derivations of equations done by Sandler *et al.* [16] are based on the IUPAC definition of isosteric heats of adsorption, which is the difference in molar enthalpy of the bulk phase and that of the adsorbed phase. This definition of isosteric heats is the basis of the work done in

this research to have an equation that predicts the isosteric heats of adsorption as will be discussed in chapter III.

Another derivation of isosteric heats of adsorption was made by Malherbe [2]. It starts with the thermodynamic equation for a bulk mixture:

$$dU = TdS - PdV + \sum \mu_i dn_i \qquad (2.13)$$

It is also considered that the adsorbent and adsorbate combined form the solid solution (aA) [2]:

$$dU_{aA} = TdS_{aA} - PdV_{aA} + \mu_a dn_a + \mu_A dn_A \qquad (2.14)$$

where the subscript "a" refers to the adsorbate and the subscript "A" refers to the solid adsorbent. Defining a new variable:$\check{\Upsilon} = \frac{n_a}{n_A}$, then $\mu_a = \mu_a(T, P, \check{\Upsilon})$ and $\mu_A = \mu_A(T, P)$, and the following equation is developed [2]:

$$\mathrm{d}\mu_a = -\bar{S}_a dT + \bar{V}_a dP + \left[\frac{\partial \mu_a}{\partial \check{\Upsilon}}\right]_{T,P} d\check{\Upsilon} \qquad (2.15)$$

At equilibrium, the chemical potential of the components in the adsorbed phase and in the gas phase (bulk phase) are equal, then [2]:

$$\mathrm{d}\mu_a = \mathrm{d}\mu_g = -\bar{S}_g dT + \bar{V}_g dP \qquad (2.16)$$

For constant $\check{\Upsilon}$ [2]:

$$\left[\frac{dlnP}{dT}\right]_{\check{\Upsilon}} = \frac{\bar{H}_g - \bar{H}_a}{RT^2} = \frac{q_{iso}}{RT^2} \qquad (2.17)$$

where:

- $\bar{H}_g$: is the partial molar enthalpy of the adsorbate in the gas phase.
- $\bar{H}_a$: is the partial molar enthalpy of the adsorbate in the adsorbed phase.

Using equation (2.17), Malherbe [2] defines the *isosteric heat of adsorption* (which is the *enthalpy of desorption*) as [2]:

$$q_{iso} = \bar{H}_g - \bar{H}_a \qquad (2.18)$$

And he defines the *enthalpy of adsorption* as [2]:

$$\Delta H(n_a) = -(\bar{H}_g - \bar{H}_a) = -q_{iso} \qquad (2.19)$$

Sircar *et al.* [17] discussed the role of isosteric heat of adsorption in estimating the temperature change of adsorbent within an adsorber through the exothermic adsorption process and the endothermic desorption process. Adsorbent temperature is important for the estimation of the local adsorption equilibria and kinetics which control the performance of the separation processes [17].

Seader and Henley [4] compared the extent of heat released upon adsorption to the heat of vaporization, and found that heat of adsorption can be less or greater than heat of vaporization and that it changes with the extent of adsorption. They also discussed heats of adsorption of liquids (usually referred to as "heat of wetting") and found it to be significantly low compared to the heat of adsorption of gases [4].

Understanding the differences between the different types of heats of adsorption and how they are obtained is crucial to assure that any comparison is made between the same types of heats of adsorption. Model predictions of heats are better verified by comparing them to experimental measurements of heats or what is called calorimetric heats.

Calorimetry is a wide field that has been studied by different researchers, among which Hill [11] who classified different categories of heats of adsorption based on a

variety of experimental/calorimetric procedures. The differences in heats of adsorption are almost of the order of RT. This difference is considered to be almost negligible for a chemisorption process, however, it is significant in the case of physisorption. Thus, knowing exactly the type of experimental heat of adsorption data available is crucial for heat balances studies in physisorption processes [18].

The equipment that is generally used to carryout experimental measurements of heats of adsorption is the Tian-Calvet calorimeter. The literature on heats of adsorption is somewhat ambiguous on the type of heat measured experimentally. What can be concluded from the early research done in this area is that differential heats of adsorption are measured and they are the so called the calorimetric heats of adsorption. On the other hand, the isosteric heats of adsorption are calculated from adsorption isotherms (Clausius-Clapeyron equation) and not obtained experimentally. However, recent research showed that isosteric heats of adsorption can be also measured calorimetrically as explained in this section.

As most of the earlier work done on heats of adsorption classified the differential heats under experimentally obtained values and isosteric heats under calculated values, there was a need to determine the relationship between these quantities. According to the work done by Hill [11], these two values are related by the following relation $q_{iso} - q_{diff} = RT$ (constant difference at constant temperature). This relationship depends on two main assumptions as highlighted by Garbacz *et al.* [19]:

(i) Adsorbate is an ideal gas.

(ii) Adsorbent is homogenous and flat- surfaced [19].

In recent published work on calorimetric heats of adsorption, different authors discussed how a Tian-Calvet calorimeter can be used to measure isosteric heats of adsorption. Shen *et al.* [20] discussed different available techniques that can be used in order to obtain "isosteric" heats of adsorption. They defined the isosteric heats of adsorption for a pure gas as the difference between the gas molar enthalpy and the adsorbed gas differential enthalpy. There are three different methods available that can be used to predict the isosteric heats of adsorption: (1) using adsorption isotherms, (2) measuring adsorption isosteres, and (3) calorimetric measurements. [20].

The first method involves the collection of experimental data of loading and pressure at different temperatures and then the differentiation of (lnP) as a function of (1/T) at constant loading to get the isosteric heats using the Clausius – Clapeyron equation (equation 2.1) [20].

The second method is called the sorption isosteric technique (SIT) and involves also the collection of experimental data of pressures and temperatures at specific loading so that plots of (lnP) vs. (1/T) called isosteres are generated with the plot linearity as a critical condition in order to obtain isosteric heats from the slope, as shown in equation (2.1). The experimental procedure in this method involves the measurements of pressures and temperatures in a closed system of identified volume and contains a known amount of gas and amount of adsorbent, however, it has a small dead space. It is essential to minimize the dead space as it assures that almost all gas is adsorbed and that the amount adsorbed is constant for the complete isostere measurement. A critical

assumption considered in this method is that the isosteric heat is temperature - independent in the temperature range of the isostere [20].

The third method is an experimental procedure that involves calorimetric measurements using a Tian-Calvet calorimeter. Shen *et al.* [20] worked on comparing isosteric heats of adsorption by the three different methods listed above aiming to obtain a "reference system" that can be used to calibrate the calorimetric instrument in order to obtain acceptable results [20].

The Tian-Calvet calorimeter operates inside an isothermal apparatus. It comprises of heat flux meters/sensors that surround a sample cell that is placed in a heat sink within which adsorption occurs. The calorimeter also has a temperature bath to fix the sample and the heat sink temperature, a gas-controlling system that doses adsorbate for the sample, and a system to collect data. The heats of adsorption evolved during the adsorption process cause an increase in the sample temperature which leads the energy to flow through the sensor and to the sink to measure the flux with time. The integration of heat flux with respect to time is used to calculate the amount of heat released for a known differential amount adsorbed [21], [22].

In their work, Parrillo and Gorte [22] discussed the different parameters that should be considered when designing and operating a heat flow calorimeter, as there are significant issues related to the measurements, such as heat losses and the time needed to reach equilibrium in the calorimeter. They also discussed the fact that the Tian-Calvet calorimeter is not only used to measure differential heats of adsorption, but can also be used to measure other types of heats as well. The type of heat measured by the

calorimeter depends on its design. In the case of sending the gas dose to the cell at the same temperature of the cell itself and sending an exact molar amount to a reference cell, then the calorimetric heat is the isosteric heat of adsorption. If the adsorbate dose enters the sample cell via a capillary tube to fix the temperature of the expanding gas, the calorimetric heat is the differential heats of adsorption [22].

Sircar *et al.* [17] discussed in their work how to experimentally measure the isosteric heats of adsorption using a multicomponent differential calorimetry (MDC). In this case, the collected isosteric heats can be used to describe the non-isothermal behavior of real adsorbers [17].

In order to assure an accurate operation of the calorimeter it is really crucial to carefully work on the sample cell design and the measurements conditions. One of the main targets in this procedure is to minimize heat losses that take place during adsorption and so, it is vital to collect the generated heats immediately and rapidly to reduce the amount of heat lost [22].

The calibration of the calorimeter is important and it can be done by either doing a chemical calibration using an adsorbent and adsorbate with an identified heats of adsorption or by doing physical calibration using Joule-effect devices [23].

In addition to the calorimeter details discussed above, a work done on heats of adsorption should explore other different factors that affect heats. Some of these factors can be adsorbent crystal structure and ion type. In addition to that, the size and the magnitude of the quadrupole moment of the gas affects heats of adsorption [21]. Some other factors, such as size and shape of the adsorbate molecules, the energetic

heterogeneity of the adsorbent, and the density of the adsorbent framework have their effect on heats of adsorption [18].

The relationship between pore size of zeolite and heats of adsorption differ between polar and nonpolar compounds. For "nonpolar" compounds, the dispersion energy increases as the zeolite pore size decreases and they are dominant. For polar (or quadrupole) molecules, between the multipole and moments of the adsorbate molecules and the electric field inside the adsorbent, there are rigorous electrostatic interactions. The ion-quadrupole interactions have substantial input to the total gas-solid interactions energy [21].

Heats of adsorption also experience a dependence on temperature that differs between porous and non-porous adsorbents. Heats of adsorption depend largely on temperature and isosters should be plotted using a second order polynomial approximation in case of porous adsorbents. Moreover, heats of adsorption have small dependence on temperature and isosters can be estimated as straight lines in case of non-porous adsorbents [19].

The applications of heats of adsorption are many, two of which were discussed by Dunne *et al.* [18]. The first application is the use of heats of adsorption profile to identify the extent of energetic heterogeneity related to the gas-solid interactions. A non-heterogeneous adsorbent towards a specific gas experiences an increase in heats of adsorption with increased loading with constant gas-solid interaction energies. This increase is a result of supportive interactions between adsorbed molecules. A highly heterogeneous adsorbent experiences a decrease in heats of adsorption with increased

gas loading with a widespread of gas-solid interaction energies. A homogenous adsorbent experiences a constant heats of adsorption profile with increased gas loading due to the equal strength of supportive gas-gas interactions and extent of gas-solid interactions heterogeneity. The second use of heats of adsorption is in the energy balance calculations of adsorption columns. As most of these columns operate under adiabatic conditions, heats of adsorption help in getting the temperature profile inside adsorption columns. This is significant, as the heats of adsorption are used to determine the regeneration energy that is considered as the highest operating cost of these columns [18].

2.5. Adsorbed phase specific heat capacity

The adsorbed phase specific heat capacity estimation is important for adsorption process modeling and researchers have been working on developing models that can be used to calculate this heat capacity from adsorption thermodynamics and equilibrium data. There have been inconsistencies in the available explanations of adsorbed phase heat capacity in literature as it is frequently assumed to be equal to the bulk phase heat capacity of the adsorbate [24].

The adsorbed phase specific heat capacity is in close relationship to isosteric heats of adsorption as the difference between the specific heat capacity of the adsorbed phase and that of the gas phase is presented by the change of isosteric heats of adsorption with temperature at constant loading [20], [25], [26], [27]. The effect of temperature on isosteric heats of adsorption is not really known as was discussed by

Shen *et al.* [20]. Most of the earlier work on this topic showed that isosteric heats are constant over some range of temperature, however, the accuracy of this claim is not clear [20]. Some researchers showed that the dependency of isosteric heats on temperature depend on adsorbent geometry, as discussed in the previous section.

The thermodynamic definition of adsorbed phase heat capacity is the derivative of the adsorbed phase enthalpy "h_a" with temperature at constant loading [27]:

$$c_{p,a} = \left[\frac{\partial h_a}{\partial T}\right]_n \tag{2.20}$$

And since isosteric heats of adsorption is defined as the difference between the gas phase enthalpy and adsorbed phase enthalpy (as discussed in previous section) then, the difference in specific heat capacity between the adsorbed and gas phases can be presented by the following equation[20],[25],[26], [27]:

$$\Delta c_n = c_{p,a} - c_{p,g} = -\left[\frac{\partial q_{iso}}{\partial T}\right]_n \tag{2.21}$$

where *n* refers to the loading, $c_{p,a}$ is the adsorbed phase specific heat capacity, and $c_{p,g}$ is the gas phase specific heat capacity.

As explained by Rahman *et al.* [27], the adsorbed phase specific heat capacity changes with temperature, pressure, and adsorbate loading, however, the gas phase specific heat capacity changes with pressure and temperature only [27]. Al Muhtaseb and Ritter [25] developed a model to estimate the adsorbed phase specific heat capacity and showed that it depends on temperature, surface coverage, adsorbent heterogeneity, and weakly on lateral interactions. The value of Δc_n depends upon the type of adsorbent used, the adsorbate molecules, and the interactions between them [28]. If the adsorbate-

adsorbent system experienced a weak adsorption then Δc_n will be almost zero indicating that the adsorbed phase heat capacity equals the gas phase heat capacity of the adsorbate. On the other hand, if the adsorbate-adsorbent system experiences a strong adsorption then the value of Δc_n will be significant. Walton and LeVan [24] concluded from their work on the same topic that the values of the adsorbed phase specific heat capacities depend largely on the adsorption isotherm model used [24].

2.6. Adsorbent selection

The selection of adsorbent material is a key factor to the high performance of adsorption separation processes. The selection process is not easily done and has a certain level of complexity. The equilibrium isotherm is the prime scientific basis for sorbent selection, and adsorbate diffusion rate is considered to be a secondary factor in significance [29]. The main characteristic of a good adsorbent is to have large specific internal volume and surface area that are accessible to the adsorbate molecules. Usually, good adsorbents have specific internal surface areas in the range between 300 and 1200 m^2/g. This specific internal surface area is a collection of pores from different sizes and channels. The adsorbent should be of good mechanical properties like the resistance to attrition and strength, in addition to having good kinetic properties to allow the transfer of adsorbate molecules promptly to the adsorption sites. There are different types of highly porous solids that can be classified as good adsorbents such as carbonaceous, inorganic, synthetic, and natural materials [30].

When designing an adsorption separation process, there are some important considerations related to the adsorbent. These design considerations are discussed by Yang [29] and they are: the capacity of the adsorbent, the method used to regenerate the adsorbent, the length of the unused bed, and the required product purities [29]. Among the different types of available adsorbents, some are selectively used in industry such as activated carbons, activated clays, silica gel, silicates, natural zeolites, synthetic zeolites, activated aluminas, and molecular sieves. Hydrophobicity is a main physical property of every adsorbent and it is a key factor that must be considered when selecting the appropriate adsorbent for a certain adsorption system. A hydrophilic adsorbent has a polar surface, and due to this, it adsorbs highly polar molecules such as water. A hydrophobic adsorbent has a non-polar surface and, therefore, adsorbs non-polar components [31].

The focus of this work is on zeolites as adsorbents. They are used in industrial separation processes because it is feasible to manufacture them to meet the specific requirements of certain processes. In addition to that, zeolites have the characteristic of regular cavity shape and size which makes them a good choice for the observation of confinement effects in adsorption equilibrium [13].

2.6.1. Zeolites

Zeolites can be defined as crystalline aluminosilicates that contain alkali or alkali earth elements, like potassium, sodium, and calcium. They are represented by the following chemical formula [29]:

$$M_{x/n}\left[(AlO_2)_x(SiO_2)_y\right].zH_2O$$

where:

- M: is the cation that occupies the sites of the zeolite.
- x and y: are integers and the ratio y/x is equal to or greater than 1.
- n: is the valence of cation M.
- z: is the number of water molecules in each unit cell [29].

As described by Yang [29], zeolites consist of tetrahedral main structural units that contain silica and alumina, SiO_4 and $A1O_4$. These units are gathered to form a secondary polyhedral that forms units like cubes, hexagonal prisms, octahedra, and truncated octahedra. The silicon and aluminum atoms are positioned at the corners of the polyhedral and are linked by a shared oxygen atom. The last structure of the zeolite is basically an assembly of the secondary units that forms a three-dimensional crystalline framework. The micropore structure of the zeolite is determined by the crystal lattice and, due to this, it is highly uniform and has no pore size distribution like other types of adsorbents [3].

There are many available types of zeolites, natural and synthetic. However, the three main types for industrial adsorption processes are types A, X, and Y. Type A zeolite is usually referred to as Linde Type A or LTA while types X and Y are referred to as faujasite or FAU. Type A zeolite is usually synthesized in Sodium form and comes in different types (depending on the type of ion exchange) such as type 4A that has effective window aperture size of around 3.8 Å and sites occupied by Sodium cations. Another A type is 3A zeolite that has an effective aperture size of 3.0 Å and sites

occupied by K^+ instead of Na^+. Zeolite 5A is one of the most commercially used in gas adsorption separation processes and it has an unimpeded apertures of a size of 4.3Å and sites occupied by either Ca^{+2} or Mg^{+2} [29].

The main focus of this research is on zeolites that have nearly spherical structure. Some of them were presented by D'Lima [13] such as, chabazite, deca-dodecasile 3R, zeolite 13X, zeolite A, zeolite L, ZIF-8 (sodalite), ZIF-90 (sodalite), ZIF-Cl (sodalite), ZIF-COOH (sodalite), ZIF-NO2 (sodalite) [13]. The structure of some of these zeolites and their figures are approximated by Zeomics [32] as shown in Figures 2 - 4.

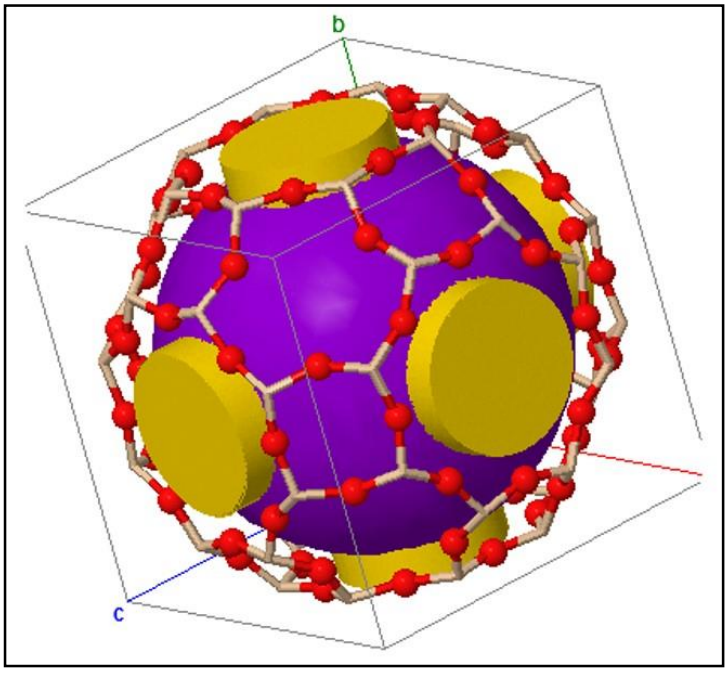

Figure 2: LTA zeolite structure as approximated by Zeomics, reprinted with permission from [32]

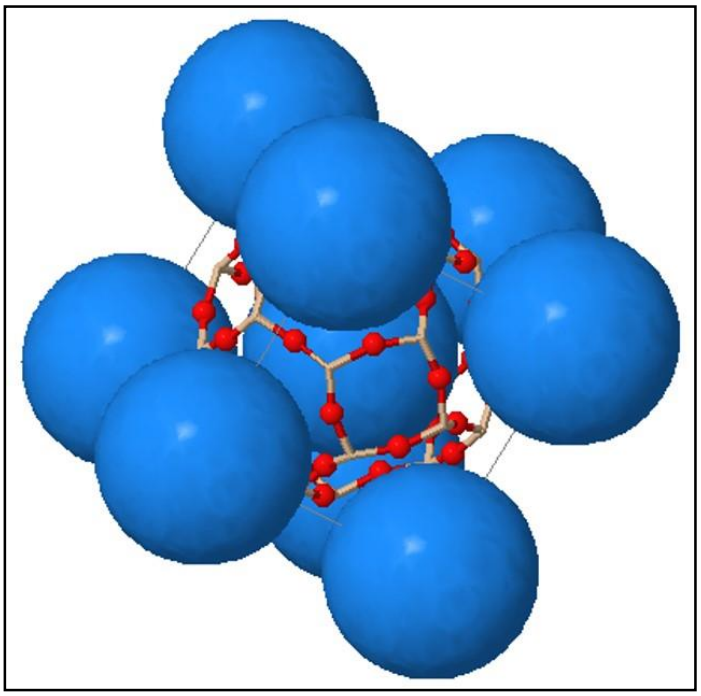

Figure 3: Sodalite zeolite structure as approximated by Zeomics, reprinted with permission from [32]

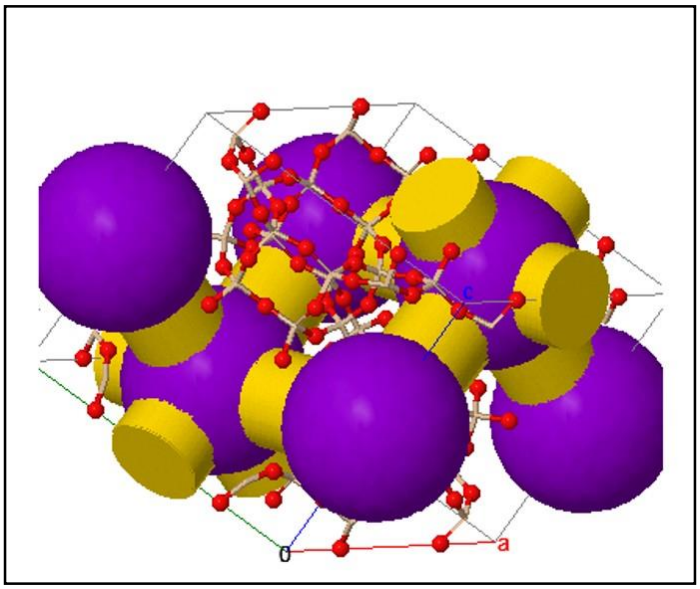

Figure 4: Chabazite zeolite as approximated by Zeomics, reprinted with permission from [32]

Some of these zeolites (with spherical structure) will be used in this work in order to fit adsorption isotherms and predict heats of adsorption for the adsorption of different pure gases. The main focus will be on types 'A' and 'X' zeolites as there is much published work on the adsorption of different gases on these types of zeolites. This makes them good selections for model testing and heats of adsorption predictions [33].

Zeolite A has approximately spherical pores, in addition to cylindrical structures that connect the spherical pores. Zeolite 5A is one of the zeolites selected in this work. Its free aperture of pores opens the path for molecules that have a kinetic diameter that is smaller than 4.9 Å [33]. The structure of zeolite A consists of a cube that has a pseudo cell consisting of eight sodalite cages positioned at the corner of the cube; this forms a large polyhedral alfa cage that has a free diameter of 11.4 Å. When these units are placed in a cubic lattice, it gives a 3D isotropic channel structure bounded by eight membered oxygen rings [3]. Zeolite A has twelve univalent exchangeable cations in each cell [3]. Their type and position affect the type of the zeolite, as their change modifies the channel size and the properties of the zeolite like its selectivity towards a specific component. Changing the framework structure type, the type of exchangeable cations, and the Si/Al ratio helps in manufacturing different types of zeolites with different adsorption properties. In zeolite A, different types of exchangeable cations are available, such as Na, Ca, and K, and with each of them the zeolite has different effective channel diameters. The main uses of zeolite A in industry are in pressure swing adsorption used for hydrogen purification, cracked gas drying, CO_2 removal from natural gas, air separation, and linear paraffin separation [30].

The structure of zeolite X is a unit cell which is composed of an eight cages array that contains around 192 tetrahedral units of AlO_2 and SiO_2. The framework of this zeolite is basically a tetrahedral lattice of sodalite units that are connected via six membered oxygen bridges, resulting in a channel structure that is widely open. Each cage in this zeolite is connected to four other cages via twelve membered oxygen rings of a 7.4 Å free diameter [3]. In zeolite X, different types of exchangeable cations are available such as Ca, Sr, Ba, and Na, and with each of them the zeolite has different effective channel diameters. The main applications of zeolite X in industry are in xylene separation and removal of mercaptans from natural gas [30].

The cation type in the zeolite affects not only its structure and properties but also the heats of adsorption. This effect depends on the cation type and the type of the adsorbate molecules. For quadrupole adsorbate molecules, the cation type has a huge effect on heats of adsorption, however, the effects are less prominent at higher loadings [21]. For non-polar adsorbate molecules, the cation type has less effect on heats of adsorption, but it increases heats of adsorption at low adsorbate loadings. Some zeolites with small pore size experience heat of adsorption that is higher than that observed in large pore size zeolites for the same adsorbate due to the increased dispersion energy in small pore size zeolites [21].

This work considers both types of zeolites (A and X) to be purely spherical and that the effect of any cylindrical pores in them to be negligibly small, as done by D'Lima [13].

CHAPTER III

RESEARCH METHODOLOGY

3.1. Model description

The starting point of the model used in this work was the research done by Travalloni *et al.* [1] in extending the van der Waals equation of state for the modeling of confined fluids in cylindrical pores. In their work, Travalloni *et al.* assumed that the interactions between the molecules of the fluid and the pore wall follow the square-well potential. The work of D'Lima [13] developed the work done by Travalloni *et al.* [34] on van der Waals theory and extended the Peng-Robinson equation of state to be used for spherical pores geometry.

According to the work done by D'Lima [13] on model development for spherical pore geometry, the model does not represent an individual molecule in a single pore, but it represents that behavior of many molecules in many pores [13]. The model developed by D'Lima [13] is used in this work for the calculations of gas adsorption equilibrium in order to correlate and predict adsorption isotherms of fluids confined in spherical pores. The model was further applied on this research to calculate the calorimetric adsorption properties by estimating the isosteric heats of adsorption of pure gases adsorbed on solid adsorbents.

3.2. Model development

3.2.1. Equation of state

The equation of state used in this work was formulated to represent the bulk and the adsorbed phases. This aims to decrease the conceptual complexity of the adsorption equilibrium calculations, which normally use different models for the bulk and adsorbed phases. In order to use the same equation of state for both bulk and confined phases, the bulk phase is simulated as a system that is confined by an extremely large pore of non-interacting walls in order to eliminate the effect of the wall on the molecules [13].

Travalloni *et al.* [34] developed an expression for the extended the Peng-Robinson equation of state for fluids confined in cylindrical pores (PR-C), which is as follows [13], [34] for pure components:

$$P = \frac{RT}{v - b_p} - \frac{a_p(T)}{v\left(v + b_p\right) + b_p\left(v - b_p\right)} - \theta \frac{b_p}{v^2}\left(1 - \frac{b_p}{v}\right)^{\theta - 1}\left(1 - F_{pr}\right)\left(RT\left(1 - \exp\left(-\frac{N_{av}\varepsilon_p}{RT}\right)\right) - N_{av}\varepsilon_p\right) \quad (3.1)$$

where:

- R: is the universal gas constant.
- a_p: is the confinement-modified energy parameter of the fluid mixture.
- b_p: is the confinement modified volume parameter.
- v: is the molar volume of the fluid.
- F_{pr}: is the fraction of confined molecules in the square-well region of the pores for random distribution of the fluid.
- N_{av}: is Avogadro's number.

- ε_p: is the square well depth of the molecule-wall interaction potential.
- θ: is the geometric factor [13], [34].

The model developed by D'Lima [13] for adsorption equilibrium calculations of confined fluids in spherical pores follows equation (3.1). The models of Travalloni *et al.*[34] and D'Lima [13] only differ in the expressions used for a_p, b_p, F_{pr}, and θ. D'Lima's [13] model used in this work correlates and predicts adsorption isotherms for different pure gases on different types of zeolites.

Component fugacities, molar volume, adsorbed amount, and residual properties in bulk and confined phases are calculated using this model. After fitting the model's parameters by comparison with experimental equilibrium isotherms, heats of adsorption are predicted using the model and compared to experimental calorimetric data and calculated isosteric heats using Clausius – Clapeyron equation.

The calculations were carried out in Excel using Visual Basic functions developed during D'Lima's [13] work. The input arguments of these functions are: the universal gas constant, pressure, temperature, mole fraction, and the properties of the substance such as critical temperature T_c, critical pressure P_c, acentric factor ω and the binary interaction parameter k_{ij} (which is zero for pure components) [13]. Spreadsheet calculations are done for both the confined phase and the bulk phase. Experimental data obtained from different references are also included in the spreadsheet for data fitting and comparison with model results.

Since the calculations are done for the adsorption of pure components on zeolites, three important "confined phase" characteristic properties are needed; the energy parameter ε_p, the size parameter δ_p/σ, and the pressure inside the pores.

Obtaining these parameters is a challenging task as it involves many trials of calculations to find the combination of these three characteristic properties that gives the best fit of the model to experimental data while satisfying the phase equilibrium conditions.

3.2.2. Isosteric heats of adsorption for pure components

The derivations made to predict the isosteric heats of adsorption for pure components start with the main assumption that *there is one adsorbed phase in a single pore and one bulk phase in the adsorption system (bulk + adsorbed phases)*. The isosteric *heats* of adsorption (q_{iso}) of a pure component is defined as the difference in molar enthalpy of the pure component in the bulk phase h^b and that in the adsorbed phase h^a [16]:

$$q_{iso} = h^b - h^a \qquad (3.2)$$

As discussed before, in order to have phase equilibrium between the bulk and the adsorbed phases, the chemical potential of both must be equal:

$$\frac{\mu^a}{RT} = \frac{\mu^b}{RT} \qquad (3.3)$$

Differentiating equation (3.3) with temperature at constant loading results in:

$$\left(\frac{\partial\left[\frac{\mu^a}{RT}\right]}{\partial T}\right)_{v^a} = \left(\frac{\partial\left[\frac{\mu^b}{RT}\right]}{\partial T}\right)_{v^a} \qquad (3.4)$$

As shown from equation (3.4), the derivative is taken at constant molar volume of adsorbed phase, but since the volume of the pores of the adsorbent is fixed, the loading (mol/kg) is constant and constant molar volume (v^a) of adsorbed phase. Expressing the above property change in terms of changes in adsorbed phase pressure (p^a) and temperature (T) results in:

$$\left(\frac{\partial\left[\frac{\mu^a}{RT}\right]}{\partial T}\right)_{v^a} = \left(\frac{\partial\left[\frac{\mu^a}{RT}\right]}{\partial T}\right)_{p^a}\left(\frac{\partial T}{\partial T}\right)_{v^a} + \left(\frac{\partial\left[\frac{\mu^a}{RT}\right]}{\partial p^a}\right)_{T}\left(\frac{\partial p^a}{\partial T}\right)_{v^a} \qquad (3.5)$$

Equation (3.5) can be written similarly for the bulk phase fluid as follows:

$$\left(\frac{\partial\left[\frac{\mu^b}{RT}\right]}{\partial T}\right)_{v^a} = \left(\frac{\partial\left[\frac{\mu^b}{RT}\right]}{\partial T}\right)_{p^b}\left(\frac{\partial T}{\partial T}\right)_{v^a} + \left(\frac{\partial\left[\frac{\mu^b}{RT}\right]}{\partial p^b}\right)_{T}\left(\frac{\partial p^b}{\partial T}\right)_{v^a} \qquad (3.6)$$

Simplifying equations (3.5) and (3.6) results in:

$$\left(\frac{\partial\left[\frac{\mu^a}{RT}\right]}{\partial T}\right)_{v^a} = -\frac{h^a}{RT^2} + \frac{v^a}{RT}\left(\frac{\partial p^a}{\partial T}\right)_{v^a} \qquad (3.7)$$

$$\left(\frac{\partial\left[\frac{\mu^b}{RT}\right]}{\partial T}\right)_{v^a} = -\frac{h^b}{RT^2} + \frac{v^b}{RT}\left(\frac{\partial p^b}{\partial T}\right)_{v^a} \qquad (3.8)$$

The next step is to substitute equations (3.7) and (3.8) in equation (3.4) results in the following:

$$-\frac{h^a}{RT^2} + \frac{v^a}{RT}\left(\frac{\partial p^a}{\partial T}\right)_{v^a} = -\frac{h^b}{RT^2} + \frac{v^b}{RT}\left(\frac{\partial p^b}{\partial T}\right)_{v^a} \qquad (3.9.a)$$

$$\frac{h^b}{RT^2} - \frac{h^a}{RT^2} = \frac{v^b}{RT}\left(\frac{\partial p^b}{\partial T}\right)_{v^a} - \frac{v^a}{RT}\left(\frac{\partial p^a}{\partial T}\right)_{v^a} \qquad (3.9.b)$$

Up to equations (3.9.a and 3.9.b), all derivations made are based on thermodynamics only with no approximation. Now, with the assumption that the bulk phase is an ideal gas, the following equation for isosteric heats of adsorption is obtained:

$$q_{iso} = h^b - h^a = RT^2 \left(\frac{\partial ln\, P^b}{\partial T}\right)_{v^a} - Tv^a \left(\frac{\partial p^a}{\partial T}\right)_{v^a} \qquad (3.10)$$

It is important to highlight that the first term of equation (3.10) - $RT^2 \left(\frac{\partial ln\, P^b}{\partial T}\right)_{v^a}$- is usually referred to as the isosteric heats of adsorption in most of the literature available on this topic. However, if the IUPAC definition of isosteric heats is used, the second term of equation (3.10) - $Tv^a \left(\frac{\partial p^a}{\partial T}\right)_{v^a}$- must be subtracted from the first term to obtain the isosteric heats of adsorption. For convenience the first term - $RT^2 \left(\frac{\partial ln\, P^b}{\partial T}\right)_{v^a}$- is referred to as "pseudo-isosteric" heats of adsorption ($q_{p\text{-}iso}$).

The calculations made with this work's model will involve the calculation of both of the pseudo-isosteric heats and isosteric heats of adsorption. A comparison between obtained pseudo-isosteric heats of adsorption and calorimetric heats as well as heats predicted from Clausius – Clapeyron equation is made since both are based on equation (3.11):

$$q_{p-iso} = RT^2 \left(\frac{\partial ln\, P^b}{\partial T}\right)_{v^a} \qquad (3.11)$$

$$q_{iso} = q_{p-iso} - Tv^a \left(\frac{\partial p^a}{\partial T}\right)_{v^a} \qquad (3.12)$$

Pseudo-isosteric heats are obtained by introducing a "disturbed temperature, T^*" for each (T, P) point involved in calculations. This disturbed temperature $T^* = T + 1K$. The procedure is to make all calculations for this disturbed temperature and then obtain

the pressures of the bulk and adsorbed phases at this temperature by trial and error. The solution for both pressures must satisfy the condition of minimizing the squared difference between the adsorbed amount at T and T^* as well as the squared difference in between the bulk and the adsorbed phases fugacity at T^*.

Since the model used in this research is structured to calculate the residual properties of the enthalpies of both of the bulk and the confined phases, the calculations of isosteric heats of adsorption are done using these properties as well as shown from equation (3.13):

$$q_{iso} = h^b - h^a = \left(h^{b,R} + h^{b,ig}\right) - \left(h^{a,R} + h^{a,ig}\right) \qquad (3.13)$$

For a pure ideal gas, the molar enthalpy depends only on temperature (T) and, hence:

$$h^{b,ig} = h^{a,ig}$$

This leads to equation (3.14):

$$q^{iso} = h^{b,R} - h^{a,R} \qquad (3.14)$$

where the superscript 'R' refers to the residual property and "ig" refers to the ideal gas state.

Equation (3.14) shows the simple and direct relationship that exists between the residual properties in the adsorbed and bulk phases and the isosteric heats of adsorption of a pure substance.

3.2.3. Adsorbed phase heat capacity

The adsorbed phase heat capacity calculations were done using equation 2.21. The derivative of the isosteric heats of adsorption with temperature at constant loading

was done manually using the forward, backward, and centered differentiation. For some of the systems the derivative of the isosteric heats was done based on three temperatures and for others was done using two temperatures only depending on the availability of different temperature points at the same adsorbed amount value.

3.3. Calculations procedure

The calculations performed in this work are all based on the extended Peng-Robinson equation of state for fluids confined in spherical pores. In order to perform the calculation in the Excel spreadsheet, the XSEOS [35] program is used as it has all needed built-in functions to perform the adsorption equilibrium calculations.

The spreadsheet is first set and the experimental data (adsorbed amount and bulk phase pressure) from literature are entered. Needed physical properties such as the critical temperature T_c, the critical pressure P_c, the acentric factor ω and the binary interaction parameter k_{ij} of the gas being studied are entered. In addition to all this, the geometrical information about the zeolite used such as the specific pore volume is entered in this sheet. The calculations are done on an iterative basis in which the objective function is the squared relative difference between the experimental and the correlated adsorbed amount and the target is to get this difference to a minimum value.

In order to accomplish this and in order to satisfy the adsorption equilibrium conditions (at which the calculations are performed), a main assumption is placed which is that all pores of the zeolite are of the same size. The main constraint is the equal

fugacities of the bulk and the confined phases, which is the condition of isofugacity at every pressure point, as shown in equation (3.15):

$$\sum_1^m([ln\emptyset_a + lnP_a] - [ln\emptyset_b + lnP_b])^2 = 0 \qquad (3.15)$$

where m refers to the number of data points, $\emptyset_a$ and $\emptyset_b$ are the fugacity coefficients of the adsorbed and bulk phases respectively. Similarly, P_a and P_b are pressures of the adsorbed and bulk phases respectively.

Once the calculations are done at this stage, "Solver" in Excel is used to perform the iterations in order to get the solution that satisfies the constraint above. The parameters that are changed by Excel are the confined phase pressure, the energy parameter ε_p, and the size parameter δ_p/σ.

The energy and size parameters are firstly assigned initial guesses based on literature review (if information are available) or some reasonable initial guesses based on previous successful systems done using XSEOS [35]. The calculations are done for the bulk (gas) phase by assuming a very large pore radius, and by setting the parameters ε_p and δ_p/σ equal to zero to eliminate any wall effect on the bulk phase properties. The confined phase calculations are done using the three parameters listed above. Snapshots of the Excel sheet used in this work are shown in Figures 5 - 7.

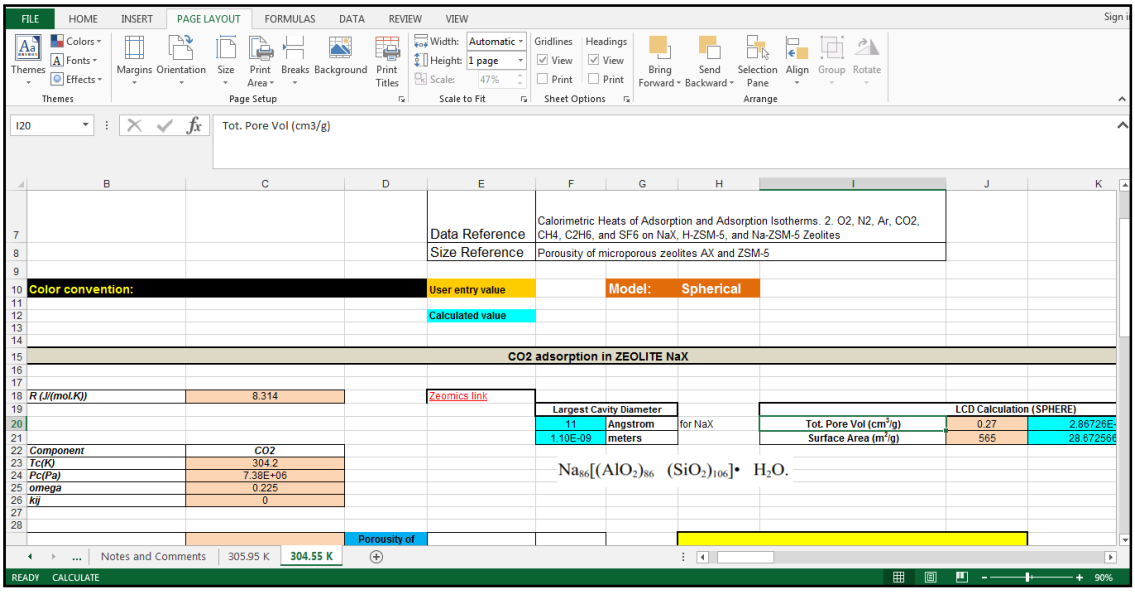

Figure 5: Snapshot 1 of XSEOS Excel sheet used in this work

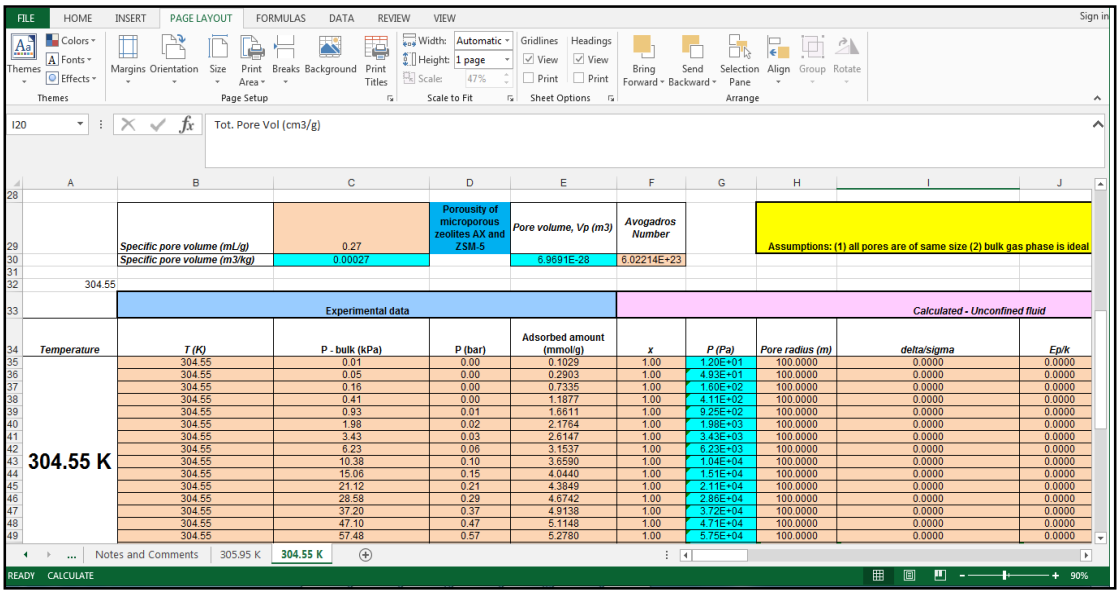

Figure 6: Snapshot 2 of XSEOS Excel sheet used in this work

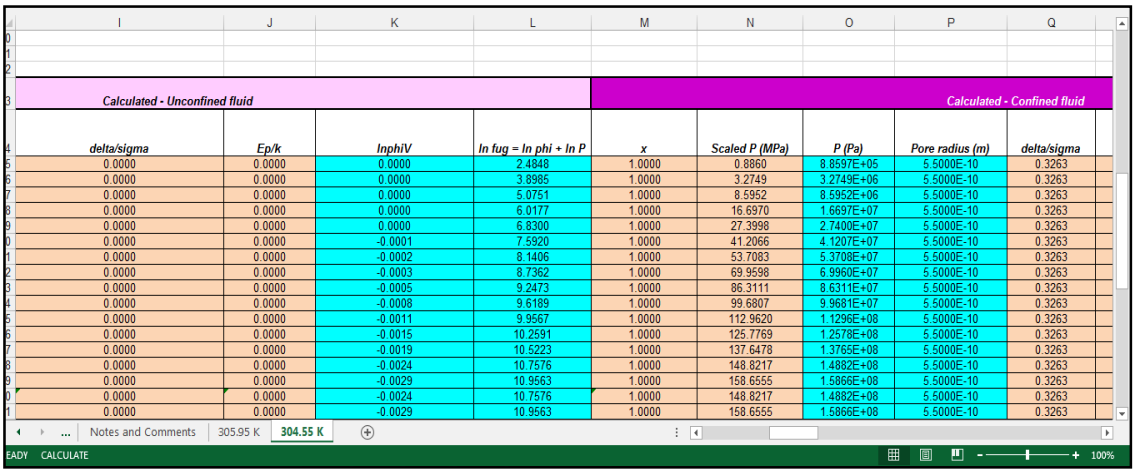

	I	J	K	L	M	N	O	P	Q
3	Calculated - Unconfined fluid				Calculated - Confined fluid				
4	delta/sigma	Ep/k	InphiV	ln fug = ln phi + ln P	x	Scaled P (MPa)	P (Pa)	Pore radius (m)	delta/sigma
5	0.0000	0.0000	0.0000	2.4848	1.0000	0.8860	8.8597E+05	5.5000E-10	0.3263
6	0.0000	0.0000	0.0000	3.8985	1.0000	3.2749	3.2749E+06	5.5000E-10	0.3263
7	0.0000	0.0000	0.0000	5.0751	1.0000	8.5952	8.5952E+06	5.5000E-10	0.3263
8	0.0000	0.0000	0.0000	6.0177	1.0000	16.6970	1.6697E+07	5.5000E-10	0.3263
9	0.0000	0.0000	0.0000	6.8300	1.0000	27.3998	2.7400E+07	5.5000E-10	0.3263
10	0.0000	0.0000	-0.0001	7.5920	1.0000	41.2066	4.1207E+07	5.5000E-10	0.3263
11	0.0000	0.0000	-0.0002	8.1406	1.0000	53.7083	5.3708E+07	5.5000E-10	0.3263
12	0.0000	0.0000	-0.0003	8.7362	1.0000	69.9598	6.9960E+07	5.5000E-10	0.3263
13	0.0000	0.0000	-0.0005	9.2473	1.0000	86.3111	8.6311E+07	5.5000E-10	0.3263
14	0.0000	0.0000	-0.0008	9.6189	1.0000	99.6807	9.9681E+07	5.5000E-10	0.3263
15	0.0000	0.0000	-0.0011	9.9567	1.0000	112.9620	1.1296E+08	5.5000E-10	0.3263
16	0.0000	0.0000	-0.0015	10.2591	1.0000	125.7769	1.2578E+08	5.5000E-10	0.3263
17	0.0000	0.0000	-0.0019	10.5223	1.0000	137.6478	1.3765E+08	5.5000E-10	0.3263
18	0.0000	0.0000	-0.0024	10.7576	1.0000	148.8217	1.4882E+08	5.5000E-10	0.3263
19	0.0000	0.0000	-0.0029	10.9563	1.0000	158.6555	1.5866E+08	5.5000E-10	0.3263
20	0.0000	0.0000	-0.0024	10.7576	1.0000	148.8217	1.4882E+08	5.5000E-10	0.3263
21	0.0000	0.0000	-0.0029	10.9563	1.0000	158.6555	1.5866E+08	5.5000E-10	0.3263

Figure 7: Snapshot 3 of XSEOS Excel sheet used in this work

The molar volume is calculated for both bulk and confined phases using the *prsvv* function that is built in XSEOS [35] excel spreadsheet as shown in equation (3.16). The calculated adsorbed amounts are estimated by multiplying the molar density (the reciprocal of the molar volume) with the specific pore volume. Once the calculations up to this stage are done, the correlated adsorption isotherms are generated by plotting the adsorbed amounts versus the bulk phase pressure for each temperature [13].

$$\text{Molar volume} = \text{prsvv}(R, T, P, X, r, \delta_p/\sigma: \varepsilon_p, T_c, P_c, \omega, k_{ij}) \quad (3.16)$$

where X is the mole fraction of the component in the bulk phase and r is the pore radius.

When the best possible fit is obtained, the next step is to predict the isosteric and pseudo-isosteric heats of adsorption. A comparison between the predicted pseudo-isosteric heats and experimental calorimetric values from literature is done for some systems and for others the comparison is done with results obtained from Clausius -

Clapeyron equation or results found by other researchers that have the same basis and assumptions of the model used in this work. Plots of predicted isosteric and pseudo-isosteric heats of adsorption vs. adsorbed amount are then generated. These isosteric heat profiles reflect the heterogeneity level of the gas– zeolite system. These profiles are compared to either calorimetric plots or literature findings for the studied systems.

When isosteric heats of adsorption are predicted using this work's model, values of isosteric heats at different temperatures for the same adsorbed amount are extracted from the obtained results and used in order to estimate the adsorbed phase heat capacity. For some systems the comparison of obtained adsorbed phase heat capacity with other researchers' calculations was possible and it was done; however, for other studied systems in this work, the comparison was not done due to the unavailability of such data. The optimum scenario would be to compare the obtained adsorbed phase heat capacity to calorimetric measurements, however, experimental measurement of adsorbed phase heat capacity of gases on zeolites studied in this work are not available.

As stated by Schwamberger and Schmidt [36], the calorimetric measurements of the adsorbed phase heat capacity are difficult to find. The reason behind this is the sensitivity in mechanical work involved in making such measurements in the laboratory. Despite the long time needed to carry out these experiments, part of it – such as the sealing of samples into a vapor-tight casing for each value of adsorbed amount - might not be done properly [36].

CHAPTER IV

CALCULATIONS, RESULTS AND DISCUSSION

This chapter explains the calculations done during this research for the different adsorbate-adsorbent systems. The systems that are used in this work are described followed by the calculations of adsorption isotherms, isosteric heats of adsorption, and adsorbed phase heat capacity. The interpretation of results is based on comparison with experimental measurements and calculated values available in the literature.

4.1. Systems description

There are ten systems studied in this work. They involve the adsorption of six different pure gases (methane, ethane, nitrogen, argon, oxygen, and carbon dioxide) on two different types of zeolites (CaA and NaX). The selection of these systems was based on the need to inspect systems with light hydrocarbons and others (N_2, O_2, CO_2, Ar) on zeolites because of the industrial interest in the separation of these gases. The simultaneous availability of adsorption isotherms and calorimetric heats of adsorption from the same reference limited the systems selected for this research. Nonetheless, it was possible to develop the calculations for these ten systems and compare them with experimental/literature values. The properties of the gases used in this work are summarized in Table 1.

Table 1: Properties of pure gases used in this research

Component	*Methane*	*Ethane*	*Nitrogen*	*Oxygen*	*Argon*	*Carbon dioxide*
T_c, *K* [37]	190.6	305.4	126.2	154.6	150.8	304.2
P_c, *MPa* [37]	4.60	4.88	3.39	5.05	4.87	7.38
Acentric factor [37]	0.008	0.098	0.04	0.021	-0.004	0.225
Kinetic diameter, Å [38]	3.758	4.443	3.64–3.80	3.467	3.542	3.30–3.94

The critical temperature, critical pressure, and acentric factor are obtained from reference [37], while the kinetic diameter values are obtained from chapter 22 of reference [38]. The kinetic diameter is an important molecular property that reflects on what type of adsorbent is proper for its separation. The kinetic diameter is determined empirically and is related to the size determined by models of molecular interactions such as Lennard-Jones [39].

The zeolites that were used in this research are CaA or 5A and NaX or 13X. A brief description of these zeolites was provided in chapter II of this thesis, and more details about them are provided in this chapter. Zeolite CaA or 5A is Linde Type A (LTA) zeolite that can be used to adsorb molecules with kinetic diameter less than 4.9 Å. The properties of CaA were looked up from different literature resources and summarized in Table 2. Figure 8 shows different images of zeolite A structure based on Zeomics approximations [32].

Table 2: Properties of zeolite CaA (5A) used in this work

Zeolite CaA (5A)	*Largest cavity diameter, Å* [40]	*Total pore volume, cm^3/g* (selected value between [32] and [40])	*Surface area, m^2/g* [40]
	12	0.24	471

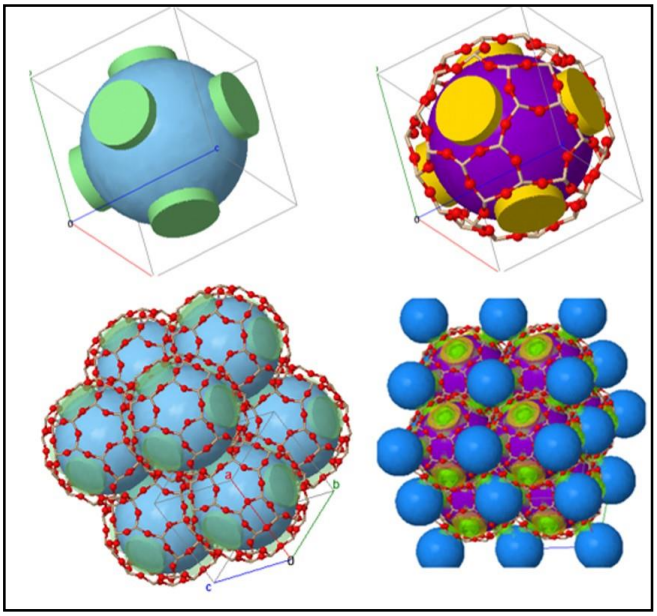

Figure 8: Structure of zeolite A from Zeomics, reprinted with permission from [32]

The other type of zeolite used in this work is zeolite NaX or 13X which is an analogue to the faujasite type of zeolite. Zeolite NaX (13X) can adsorb molecules with kinetic diameter up to 10 Å. The properties of NaX were looked up from different literature resources and summarized in Table 3. Figure 9 shows different images of the

faujasite type of zeolite based on Zeomics approximations [32]. Table 4 summarized the combination of adsorbate-adsorbent systems studied in this work.

Table 3: Properties of zeolite NaX (13X) used in this work

	Largest cavity diameter, Å [40]	*Total pore volume, cm^3/g* [40]	*Surface area, m^2/g* [40]
Zeolite NaX (13X)	11	0.27	565

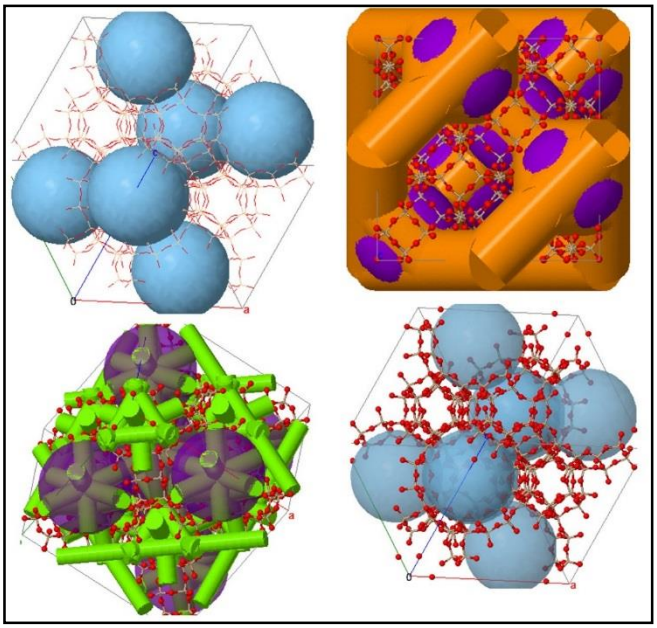

Figure 9: Structure of Faujasite zeolite from Zeomics, reprinted with permission from [32]

Table 4: Summary of systems studied in this work

System No.	*Adsorbate (gas)*	*Adsorbent (zeolite)*	*Number of isotherms*	*Reference*
1	Methane	CaA	3	[41]
2	Methane	NaX	1	[21]
3	Ethane	CaA	3	[33]
4	Ethane	NaX	1	[21]
5	Nitrogen	CaA	3	[20]
6	Nitrogen	NaX	1	[21]
7	Oxygen	CaA	3	[20]
8	Oxygen	NaX	1	[21]
9	Argon	NaX	1	[21]
10	Carbon dioxide	NaX	2	[21]

4.2. Adsorption isotherms

For the ten systems described in Section 5.1, the experimental adsorption isotherms from different references have been collected and fitted using this research's model. The results of fitted adsorption isotherms of the ten systems are presented in this section with discussion and interpretations. Experimental adsorption isotherms were used and these were fitted using the model calculations of adsorbed amount by changing the size parameter, energy parameter, and confined pressure until a satisfactory fitting that satisfies the constraint of equal fugacity of the bulk and adsorbed phase is obtained. The percentage of average relative deviation (%ARD) is calculated using equation (4.1).

$$\%\,ARD = average\left[\frac{n_{ac} - n_{ae}}{n_{ae}} \times 100\right] \qquad (4.1)$$

where n_{ac} and n_{ae} are the correlated and experimental adsorbed amounts respectively.

Adsorption usually happens at low temperatures to enhance the adsorption capacity and selectivity (in the case of mixtures). While low temperatures favor adsorption, it is generally undesirable to work a cryogenic conditions because of cost. Thus, the temperature range of adsorption processes in industry usually depends on the adsorbent-adsorbate system and the concentration of the feed. In the case of gas mixtures, the selectivity of adsorption is affected by temperature. The temperature range of the systems studied in this thesis is between 283 K and 573 K. The work done by H. Huang *et al.*[42] that discussed the effect of temperature on gas adsorption process was done at temperature range 273 – 348 K for different gases such as CO_2, CH_4, CO, and N_2 as it is the common temperature range of practical adsorption columns.

4.2.1. Adsorption isotherm(s) of methane-CaA system

The experimental adsorption isotherms of the work done by Pakseresht *et al.* [41] were used for this system. The system details and results of fitted parameters are shown in Table 5, and Figure 10 shows the experimental and the correlated adsorption isotherms of methane-CaA system.

Table 5: Methane-CaA system parameter fitting results

Temperature, K	*Bulk pressure range, kPa*	$\frac{\delta p}{\sigma}$	ε_p, *K*	*ARD, %*
303	40 – 1000	0.1889	1822.9	3.9
373	40 – 1000	0.2098	1844.0	6.1
573	40 – 1000	0.2778	1801.9	12.8

Table 5 shows that both of the size and energy parameters vary for the same adsorbate-adsorbent system, but the variation is relatively small. No trend could be obtained for the variation of ε_p, however, $\frac{\delta p}{\sigma}$ parameter increases with temperature. Figure 10, which displays the results for the adsorption of methane on CaA zeolite, shows that the correlated isotherms are of type I at the three temperatures and are in good agreement with experimental data, which is also reflected by the calculated average relative deviation in Table 5. It is interesting that the experimental isotherm at 373 K looks more like a type II isotherm; however, this might be due to experimental inaccuracies. The experimental and fitted isotherms of methane-CaA system from the work of Bakhtyari and Mofarahi [43] showed that the adsorption isotherms of this system at temperature range of 273 – 343 K is of type I isotherm.

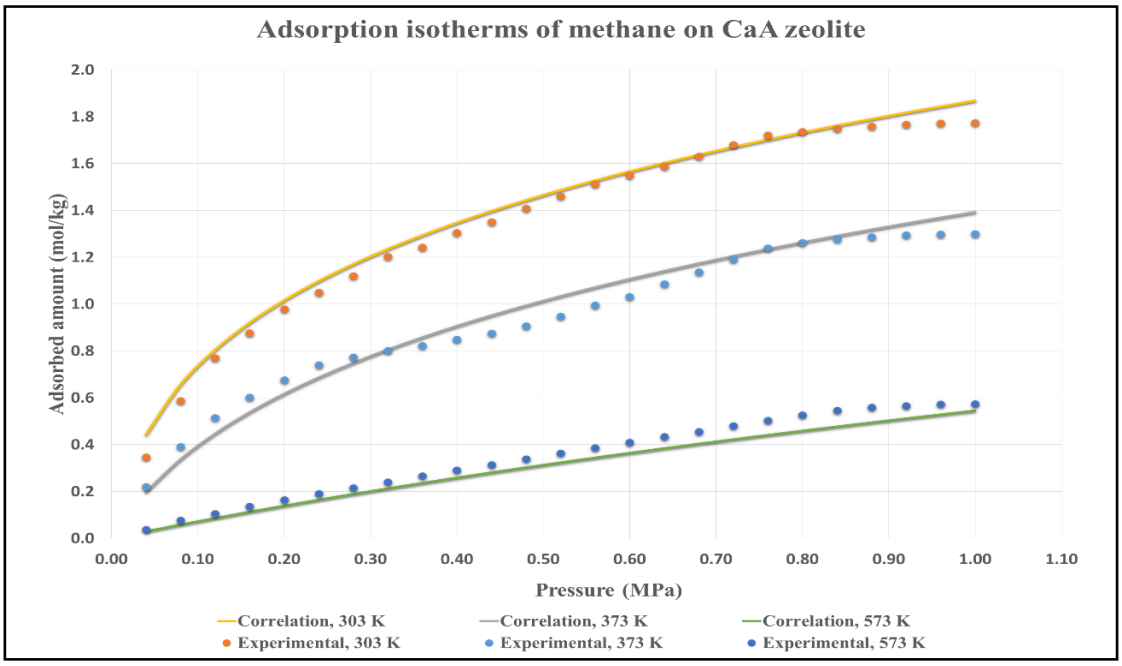

Figure 10: Experimental (adapted from [41]) and fitted adsorption isotherms of methane-CaA system

4.2.2. Adsorption isotherm(s) of methane-NaX system

The experimental adsorption isotherm of Dunne *et al.* [21] was used. Reported experimental data for methane – NaX system was available for one temperature only which was used in the correlations done using the model. The system details and results of fitted parameters, reported in Table 6 and Figure 11, show the experimental and the calculated adsorption isotherm of methane-NaX system at 304.45 K.

Table 6: Methane-NaX system parameter fitting results

Temperature, K	*Bulk pressure range, kPa*	$\frac{\delta p}{\sigma}$	ε_p, *K*	*ARD, %*
304.45	3.38 – 93.14	0.4803	1325.0	0.9530

As Figure 11 shows, the results of calculated adsorption isotherm are in very good agreement with experimental isotherm which is also reflected by the calculated average relative deviation in Table 6. Figure 11 illustrates that the adsorption of methane on NaX zeolite is of type I isotherm at 304.45 K. Since the experimental pressure range is less than the atmospheric pressure (low pressure condition), both of the experimental and calculated isotherms did not reach the adsorption saturation condition.

Comparing the results obtained for the adsorption of pure methane on both CaA and NaX zeolites from Figures 10 and 11 for the same temperature and pressure ranges, it is observed that similar amounts of methane are adsorbed on both types of zeolites.

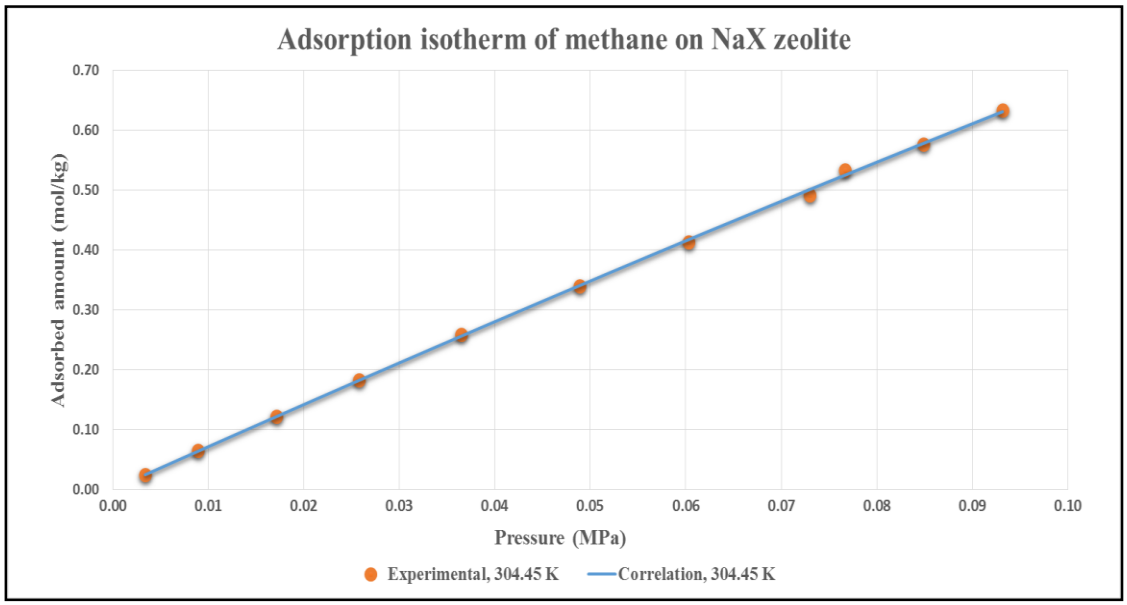

Figure 11: Experimental (adapted from [21]) and fitted adsorption isotherm of methane-NaX system

4.2.3. Adsorption isotherm(s) of ethane-CaA system

The experimental adsorption isotherms used in this system are obtained from the work done by Mofarahi and Salehi [33]. The system details and results of fitted parameters are shown in Table 7 and Figure 12 shows the experimental and the correlated adsorption isotherms of ethane-CaA system.

Table 7: Ethane-CaA system parameter fitting results

Temperature, K	*Bulk pressure range, kPa*	$\frac{\delta p}{\sigma}$	ε_p, *K*	*ARD, %*
283	8.16 – 929.6	0.1712	2951.4	15.81
303	8.60 – 944.2	0.1883	2951.9	15.12
323	12.2 – 947.6	0.1641	2952.0	11.14

As can be seen in Table 7, both of the size and energy parameters vary for the same adsorbate-adsorbent system, but the variation is relatively small. No trend could be obtained for the variation of these parameters with temperature. As Figure 12 shows, the results of correlated adsorption isotherms are in good agreement with experimental isotherms with a calculated average relative deviation of around 13%. Figure 12 shows that the adsorption of ethane on CaA zeolite is of type I isotherm at the three temperatures considered in this study. Comparing the results obtained for methane and ethane adsorption on CaA zeolite from Figures 10 and 12 for the same temperature and pressure ranges, it can be interpreted that ethane experiences a much stronger adsorption on CaA than that of methane on the same zeolite.

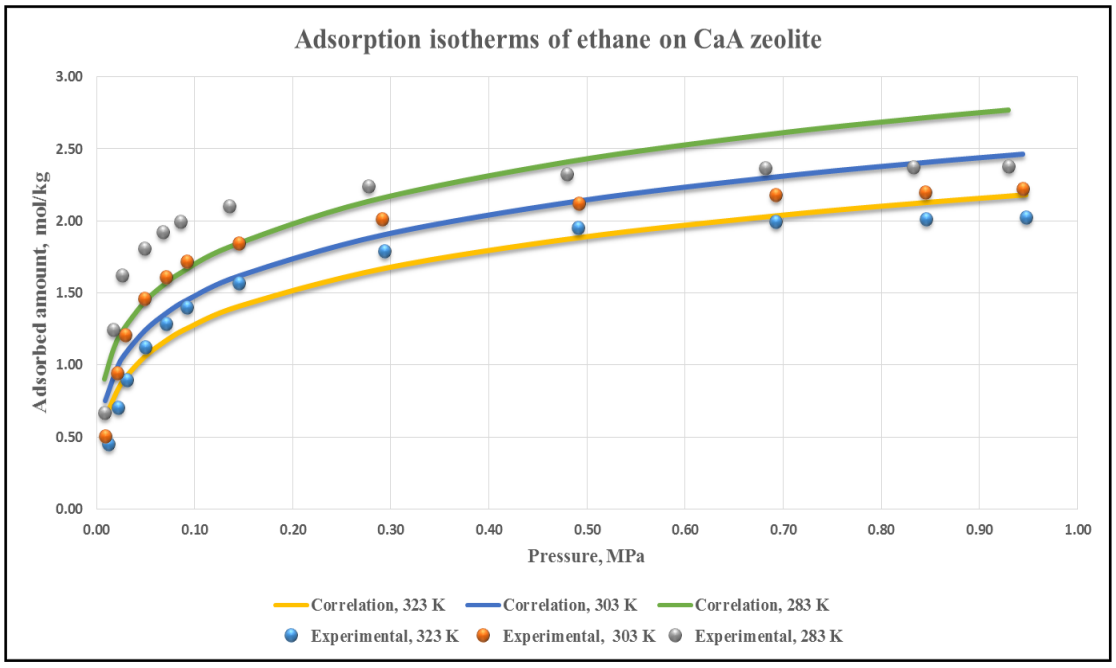

Figure 12: Experimental (adapted from [33]) and fitted adsorption isotherms of ethane-CaA system

4.2.4. Adsorption isotherm(s) of ethane-NaX system

The experimental adsorption isotherm of the work done by Dunne et al. [21] was used for this system. Reported experimental data for ethane – NaX system was available for one temperature only which was used in the calculations related to this model. The system details and results of fitted parameters are shown in Table 8. Figure 13 shows the experimental and the correlated adsorption isotherm of ethane-NaX system at 305.55 K.

Table 8: Ethane-NaX system parameter fitting results

Temperature, K	*Bulk pressure range, kPa*	$\frac{\delta p}{\sigma}$	ε_p, *K*	*ARD, %*
305.55	1.43 – 75.03	0.5938	2024.0	4.018

Figure 13 demonstrates that the adsorption of ethane on NaX zeolite is of type I isotherm at 305.55 K and there is a good agreement between the correlated and experimental results, with an error of about 4% as reported in Table 8. The experimental pressure range is less than the atmospheric pressure (low pressure condition) and, as in the case of methane-NaX system, both of the experimental and calculated isotherms did not reach the adsorption saturation condition.

Comparing the results obtained for the adsorption of pure ethane on both CaA and NaX zeolites from Figures 12 and 13 for the same temperature and pressure ranges, it can be interpreted that ethane experiences stronger adsorption on zeolite NaX than that on zeolite CaA.

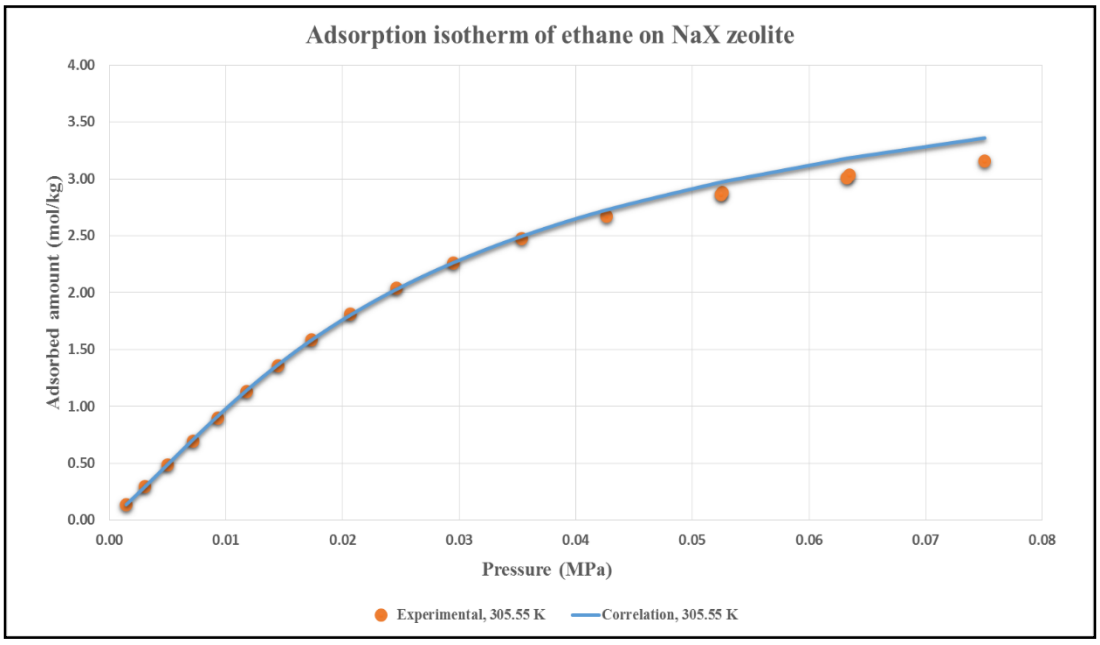

Figure 13: Experimental (adapted from [21]) and fitted adsorption isotherm of ethane-NaX system

4.2.5. Adsorption isotherm(s) of nitrogen-CaA system

The experimental data for the adsorption isotherms of nitrogen on CaA zeolite were obtained from the work of Shen *et al.* [20]. Table 9 shows the system details and results of fitted parameters. Figure 14 displays the experimental and the correlated adsorption isotherms of nitrogen-CaA system.

Table 9: Nitrogen-CaA system parameter fitting results

Temperature, K	*Bulk pressure range, kPa*	$\frac{\delta p}{\sigma}$	ε_p, *K*	*ARD, %*
308	3.05 – 125.86	0.2695	1629.8	0.9298
328	3.46 – 125.95	0.2568	1567.0	0.4498
348	3.73 – 125.56	0.2513	1515.7	0.5658

As was obtained for previous systems, and as shown in Table 9, the size and energy parameters have a small variation with temperature. For this system, the fitted values of both parameters decrease as the temperature increases. The calculated adsorption isotherms for the nitrogen-CaA system are in very good agreement with the experimental results of Shen *et al.* [20], as Figure 14 shows. The average relative deviation, presented in Table 9, is less than 1% at the three temperatures.

Both experimental and correlated isotherm indicate that the adsorption of nitrogen on CaA zeolite is of type I isotherm. Due to the low pressure conditions at which the data were collected, the adsorption saturation conditions were not obtained. Although not shown in Figure 14, the obtained results of this work are in excellent agreement with the experimental results obtained by Ertan [31].

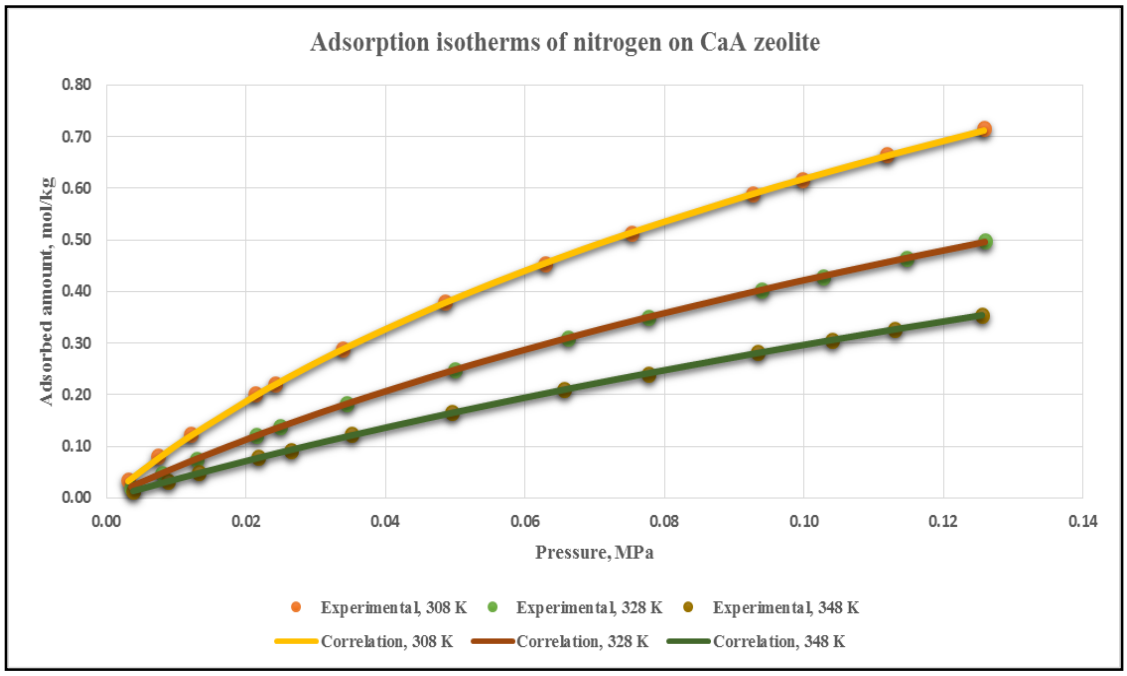

Figure 14: Experimental (adapted from [20]) and fitted adsorption isotherms of nitrogen-CaA system

4.2.6. Adsorption isotherm(s) of nitrogen-NaX system

The experimental adsorption data of Dunne *et al.* [21] were used to fit the adsorption isotherm of the nitrogen-NaX system. Reported experimental data for this system was available for one temperature only, which was used in the calculations. The system details and results of fitted parameters are shown in Table 10 and Figure 15 shows the experimental and the correlated adsorption isotherm of nitrogen-NaX system at 305.65 K.

Table 10: Nitrogen-NaX system parameter fitting results

Temperature, K	*Bulk pressure range, kPa*	$\frac{\delta p}{\sigma}$	ε_p, *K*	*ARD, %*
305.65	4.46 – 110.03	0.5027	1165.6	1.171

The fitting on Figure 15 and the average relative deviation from Table 10 show that the correlated and experimental isotherms are very close and suggest that the obtained isotherm is of type I. The obtained isotherm did not reach the saturation conditions probably due to the low experimental pressures.

Comparing the results of adsorption of nitrogen on CaA and NaX zeolites at the same temperature and pressure ranges (Figures 14 and 15), it can be noticed that nitrogen experiences stronger adsorption on CaA zeolite than on NaX zeolite.

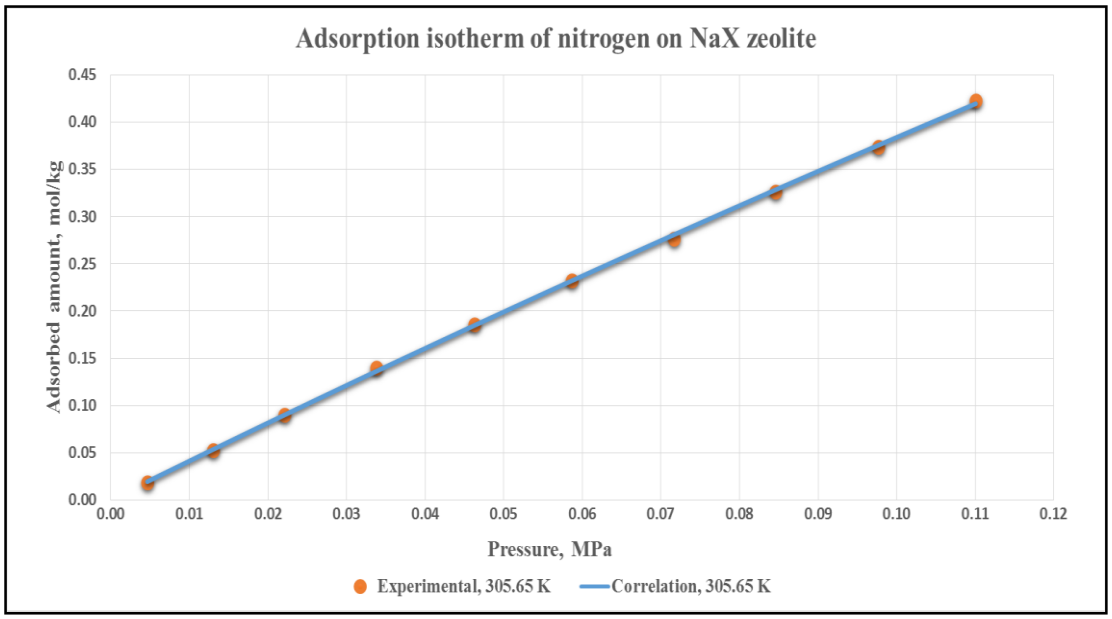

Figure 15: Experimental (adapted from [21]) and fitted adsorption isotherm of nitrogen-NaX system

4.2.7. Adsorption isotherm(s) of oxygen-CaA system

The experimental data used for the calculations and adsorption isotherms prediction for the system of adsorption of oxygen on CaA zeolite were taken from the work of Shen *et al.* [20]. The details of the system conditions and results of fitted parameters are shown in Table 11. Figure 16 displays the experimental and the correlated adsorption isotherms of oxygen-CaA system.

Table 11: Oxygen -CaA system parameter fitting results

Temperature, K	*Bulk pressure range, kPa*	$\frac{\delta p}{\sigma}$	ε_p, *K*	*ARD, %*
308	3.67 – 123.56	0.1910	1196.9	1.448
328	3.70 – 124.6	0.1670	1200.1	1.777
348	3.84 – 125.76	0.1252	1210.0	0.8211

Table 11 shows that, the size and energy parameters change with temperature. For this system, as the temperature increases, the size parameter decreases and the energy parameter undergoes a very slight increase. The fitted isotherms in Figure 16 and the calculated average relative deviation in Table 11 illustrate the good agreement between calculated and experimental results. The three isotherms did not reach the adsorption saturation condition probably due to the low-pressure conditions at which the experiment – as well as the calculations – were done.

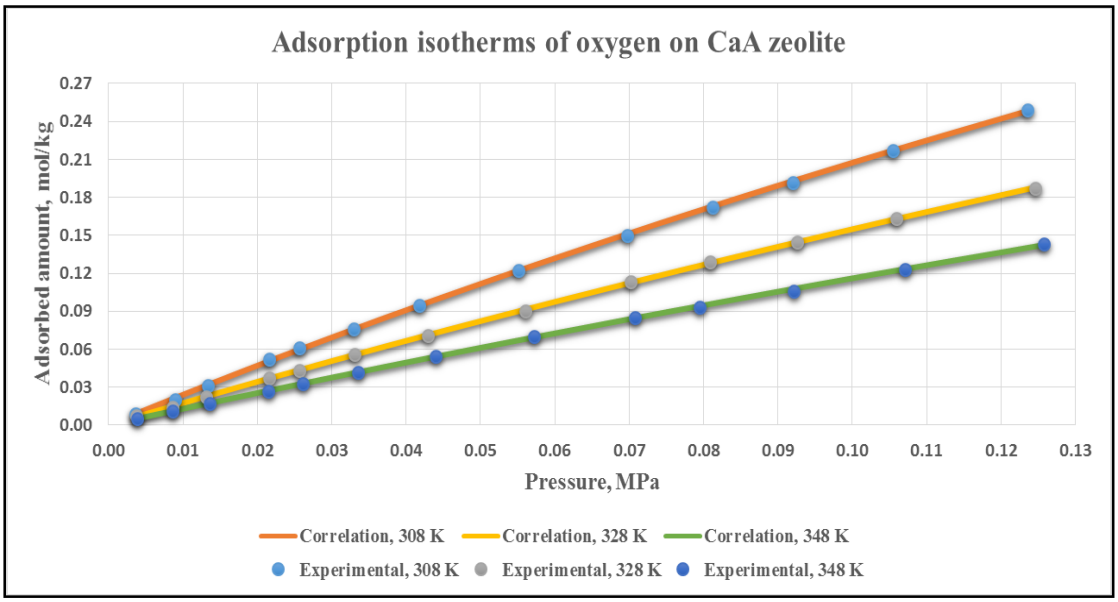

Figure 16: Experimental (adapted from [20]) and fitted adsorption isotherms of oxygen-CaA system

4.2.8. Adsorption isotherm(s) of oxygen-NaX system

The experimental results for the adsorption isotherm of oxygen on NaX zeolite from the work done by Dunne *et al.* [21] were used for the calculations and parameter fitting of this system. The details of the system and its results are shown in Table 12 and Figure 17 for the temperature of 306.35 K.

Table 12: Oxygen -NaX system parameter fitting results

Temperature, K	*Bulk pressure range, kPa*	$\frac{\delta p}{\sigma}$	ε_p, *K*	*ARD, %*
306.35	21.62 – 100.47	0.5030	759.9	1.553

The fitted isotherm from Figure 17 and the average relative deviation from Table 12 show that the calculated and experimental isotherms are very close and that the obtained isotherm is of type I. As in most of the previous systems, the obtained isotherm did not reach the saturation conditions possibly due to the low pressures of the experiment.

When the results of adsorption of oxygen on CaA and NaX zeolites are compared for the same temperature and pressure ranges (Figures 16 and 17), it can be observed that oxygen experiences stronger adsorption on CaA zeolite than that on NaX zeolite.

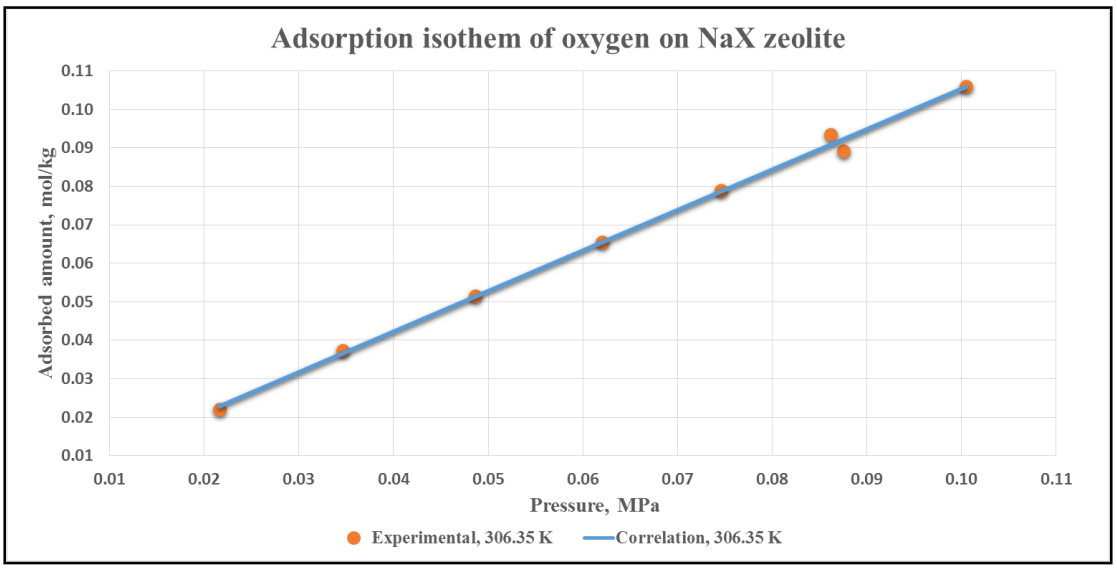

Figure 17: Experimental (adapted from [21]) and fitted adsorption isotherm of oxygen-NaX system

4.2.9. Adsorption isotherm(s) of argon-NaX system

The experimental results for the adsorption isotherm of argon on NaX zeolite from the work of Dunne *et al.* [21] were used for the calculations and parameter fitting. The details of the system and its results are shown in table 13 and Figure 18 for the temperature of 304.15 K.

Table 13: Argon -NaX system parameter fitting results

Temperature, K	*Bulk pressure range, kPa*	$\frac{\delta p}{\sigma}$	ε_p, *K*	*ARD, %*
304.15	6.24 – 96.94	0.2834	891.4	1.863

The fitted isotherm from Figure 18 and the small average relative deviation from Table 13 demonstrate that the correlated and experimental isotherms are in good agreement and that the obtained isotherm is type I. The obtained isotherm did not reach the saturation conditions probably due to the low pressure conditions of the experiment.

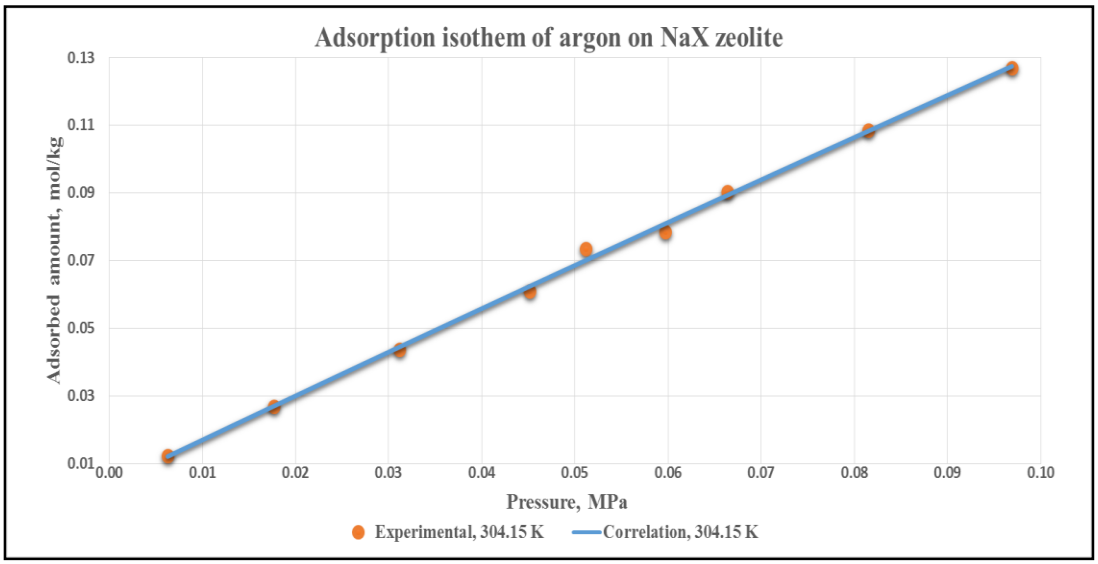

Figure 18: Experimental (adapted from [21]) and fitted adsorption isotherm of argon-NaX system

4.2.10. Adsorption isotherm(s) of carbon dioxide-NaX system

The adsorption of carbon dioxide on NaX zeolite was one of the interesting systems studied in this work as it involved several trials to get the satisfactory parameter fitting. The experimental data that were used to fit the parameters this research's model were obtained from the work done by Dunne *et al.* [21] for the adsorption of CO_2 on NaX at two temperatures. The details and results of the fitted system are shown in Table 14 and Figure 19.

Table 14: Carbon dioxide -NaX system parameter fitting results

Temperature, K	*Bulk pressure range, kPa*	$\frac{\delta p}{\sigma}$	ε_p, *K*	*ARD, %*
304.55	0.012 – 68.73	0.3216	3550.6	1.901
305.95	0.011 – 28.51	0.3274	3517.0	1.690

The obtained results from the fitting of the isotherms of this system indicates that the model isotherms are in good agreement with experimental isotherms with small calculated average relative deviation. The isotherm is of type I as Figure 19 shows.

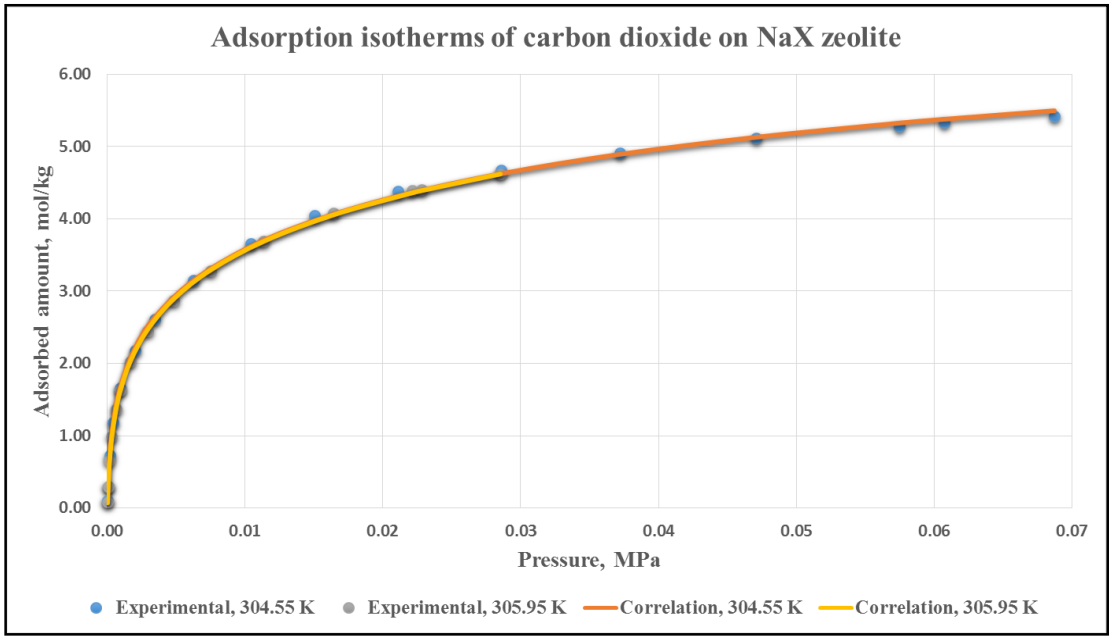

Figure 19: Experimental (adapted from [21]) and fitted adsorption isotherm of carbon dioxide-NaX system

Since for this system, the two studied temperatures are very close to each other (304.55 K and 305.95 K), another adsorption isotherm calculation was done for the same system, however, by using the energy and size parameters obtained from the correlation at 305.95 K to predict the system's behavior at 304.55 K. The result is shown in Figure 20.

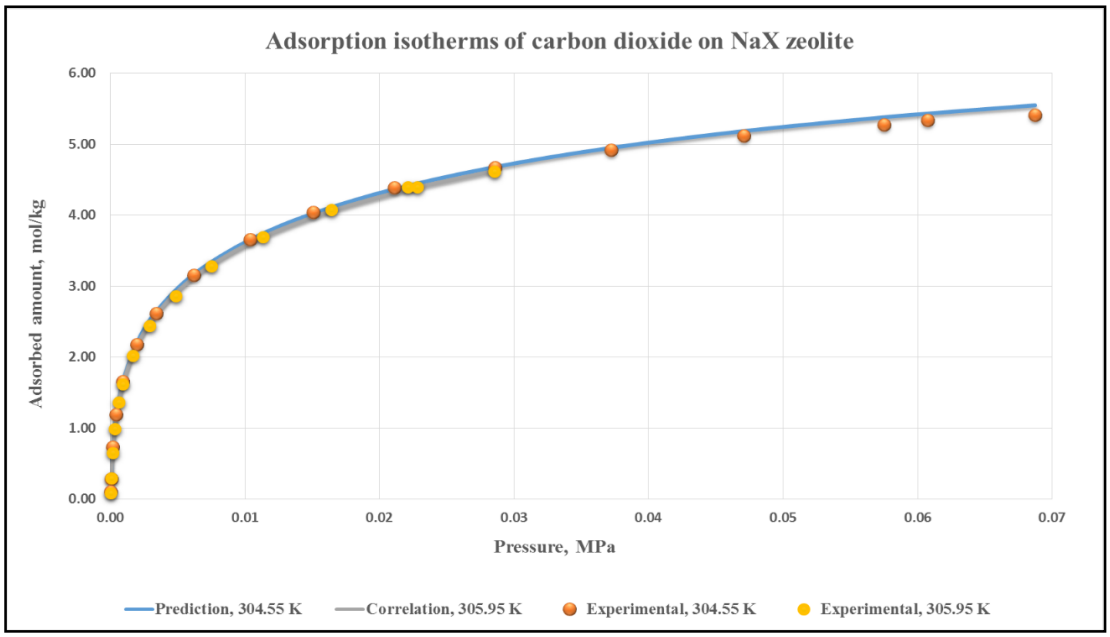

Figure 20: Experimental (adapted from [21]) and fitted adsorption isotherm of carbon dioxide-NaX system with fixed energy and size parameters. Result at 305.95 K is a correlation. Result at 304.55 K is a prediction.

As Figure 20 shows, the predicted isotherm at 304.55 K is essentially the same as the previously obtained one even though the parameters were those of 305.95 K isotherm. The new %ARD is exactly the same as the previously calculated one for the

304.55 K isotherm, which indicates that at very small temperature different, the energy and size parameters can be fixed. On the other hand, the sensitivity of energy and size parameters for temperature change was done for the adsorption of methane on CaA zeolite (system 1). The energy and size parameter obtained at 303 K isotherm were used for the 373 K isotherm, and that resulted in a predicted isotherm with a %ARD of 7.83%, which is slightly higher than the one obtained before (6.06%). Similarly, the energy and size parameters of the 303 K isotherm were used for predicting the 573 K isotherm and that resulted in %ARD of 24.6% which is almost twice the previously obtained one (12.8%). This is an indication of the sensitivity of energy and size parameter to the difference in temperature from an isotherm to another, which must be considered in the adsorption isotherms fitting of any system.

As it can be observed from the results obtained for the ten studied systems, the same pure gas experiences a stronger adsorption on a certain type of zeolite than on another. An underlying reason can be attributed to the interactions that each pure gas experiences with a certain type of zeolite which result in higher adsorption affinities. Another reason that could contribute to this observation is related to the zeolites themselves, as some have larger available pore volume per kilogram of the solid than others.

The results of the ten systems indicate that for the adsorption of the selected pure gases on CaA zeolite, ethane is the most adsorbed on CaA, followed by methane and nitrogen (with almost equal adsorption strength on CaA), and that oxygen is the least adsorbed on CaA zeolite as shown in Figure 21. The results of adsorption on NaX

zeolite points out that carbon dioxide is the most adsorbed on NaX, followed by ethane, methane, nitrogen, argon, and that oxygen is the least adsorbed on NaX zeolite as shown in Figure 22. Carbon dioxide molecules experience strong interactions with the electric field of the NaX zeolite which leads to high adsorption affinity.

This conclusion on the adsorption affinities of pure gases on NaX is in perfect agreement with what Dunne *et al.* [18] found when studying the adsorption of methane, ethane, nitrogen, oxygen, argon, and carbon dioxide on NaX. It also agrees with the results of Cavenati *et al.* [44] when comparing the adsorption of methane, carbon dioxide, and nitrogen on NaX zeolite at high pressure conditions. The obtained results reveal that oxygen and nitrogen -which are polar compounds- have higher adsorption affinities on CaA zeolite than on NaX zeolite.

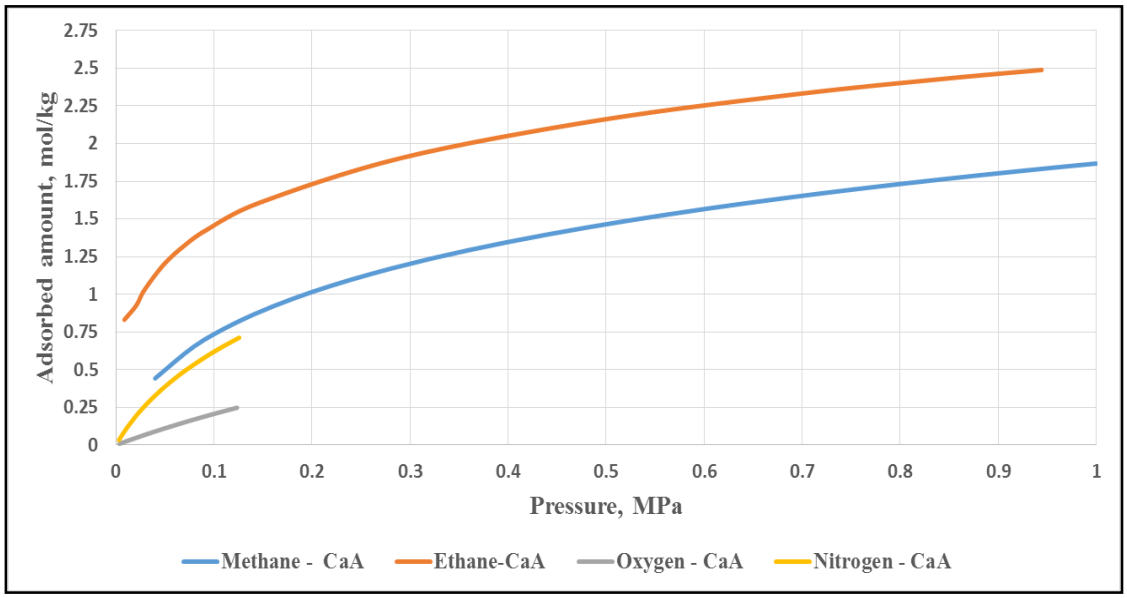

Figure 21: Adsorption isotherms of pure components on CaA zeolite, 303 – 308 K

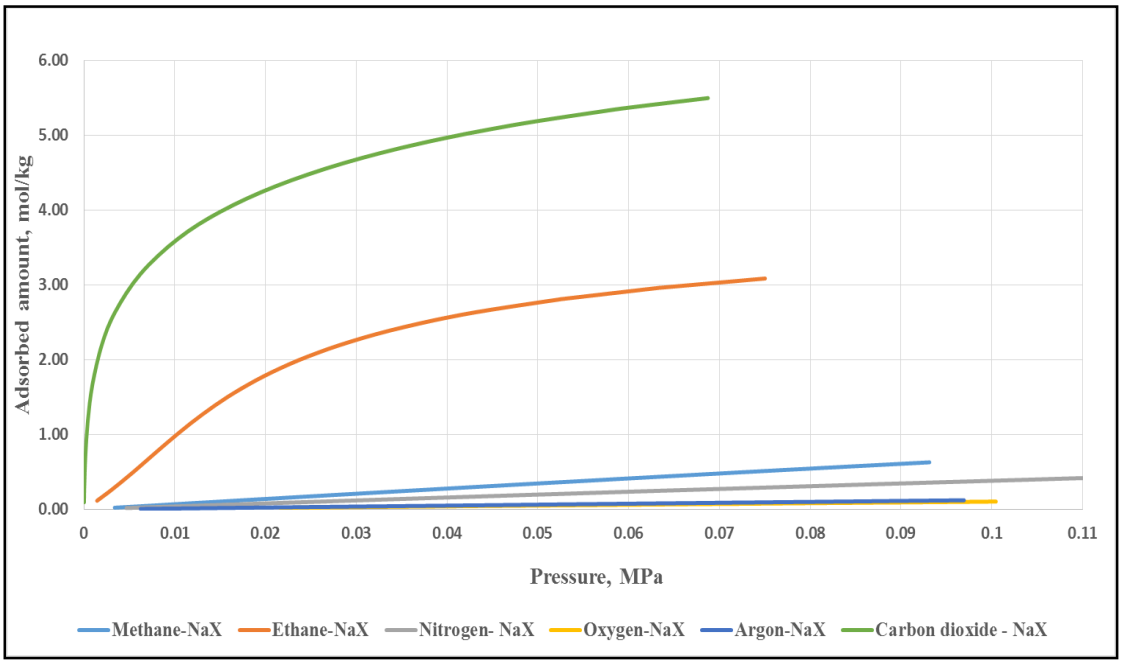

Figure 22: Adsorption isotherms of pure components on NaX zeolite, 304 – 307 K

4.3. Isosteric heats, pseudo-isosteric heats, and adsorbed phase heat capacity

For the ten systems described in Section 4.1, the isosteric heats of adsorption and the pseudo-isosteric heats of adsorption were predicted using the procedure described in Chapter III. The results were plotted as the heats of adsorption (kJ/mol) versus the amount adsorbed (mol/kg). The model results of pseudo-isosteric heats were compared to calorimetric pseudo-isosteric heats of adsorption measured experimentally and presented in the work of Dunne *et al.* [21] and the work of Shen et al. [20], and with the results from Clausius-Clapeyron equation. For systems whose calorimetric (experimental) measurements were not available, a comparison with the results from Clausius-Clapeyron equation only was made. The calculations made using Clausius -

Clapyron equation were done by using the experimental adsorption isotherms of the system and locating (graphically) three points of equal adsorbed amount and different (T,P) pairs. For each adsorbed amount value the (1/T) and (lnP) were calculated and plotted as (lnP) vs. (1/T). A linear trendline is places and the slope is take from its equation. A sample is shown in Figure 23. The slope was then used to calculate the isosteric heats of adsorption by multiplying it with (-R).

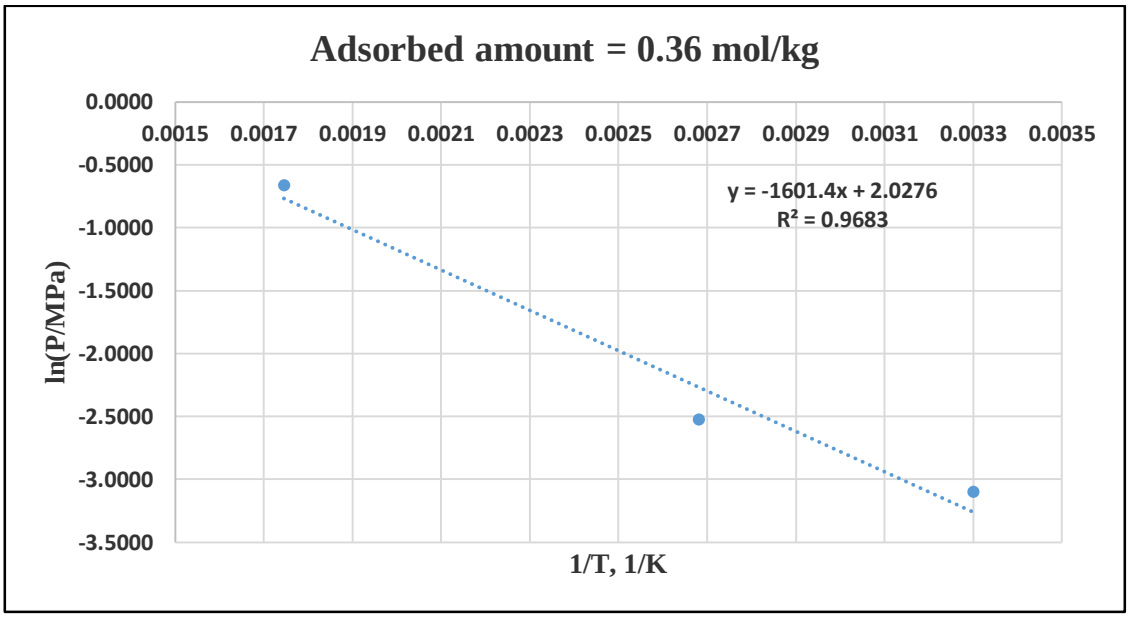

Figure 23: Sample ln(P) vs. 1/T used for Clapeyron equation calculations

For the systems with more than one isotherm, the isosteric heats of adsorption at different temperatures were used to calculate the difference in heat capacity as described in chapter III. The calculations of the difference in heat capacity between the adsorbed

phase and the gas phase were done to reflect on the temperature dependency of isosteric heats for each system.

4.3.1. Heats of adsorption of methane-CaA system

For this system, the isosteric heats of adsorption were predicted using the model's equation and plotted vs. adsorbed amount for three different temperatures as shown in Figure 24. The average isosteric heats of adsorption of methane-CaA system is around 12 kJ/mol.

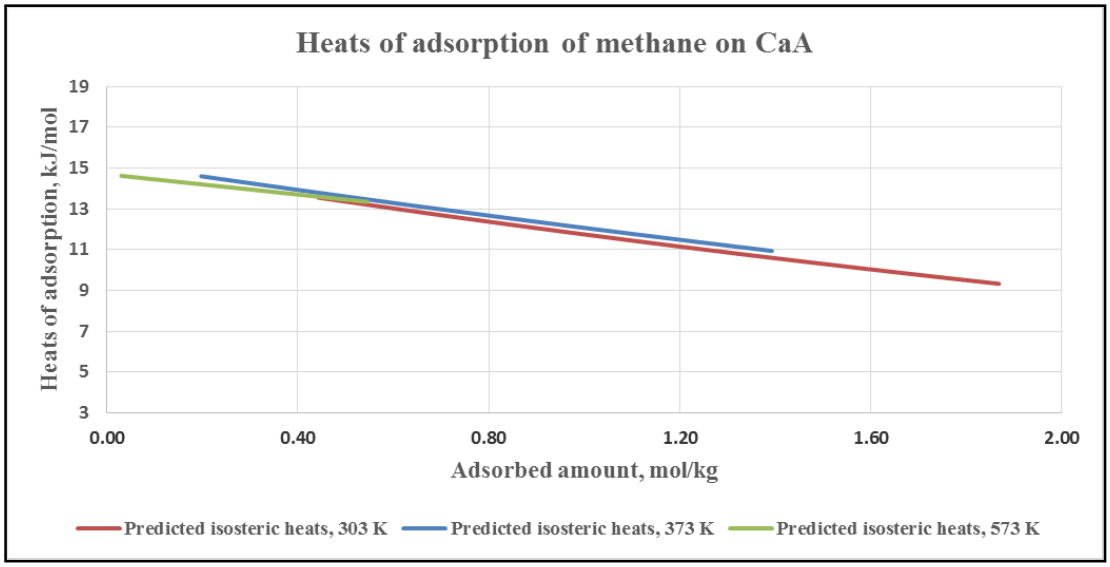

Figure 24: Model-predicted isosteric heats of adsorption for methane-CaA system

Figure 24 indicates that isosteric heats of adsorption of methane on CaA zeolite are decreasing with the adsorbed amount. This is interpreted as an indication of the effect of surface heterogeneity of zeolite CaA towards adsorption of methane molecules. The change in model-predicted isosteric heats between each two points is in the range of 0.5 – 5% with its highest at the low loading region (as shown in Figure 24). The pseudo-isosteric heats of adsorption of this system were also predicted and compared to the predicted heats using Clausius-Clapeyron equation due to the unavailability of calorimetric (experimental) measurements of these heats, as shown in Figure 25.

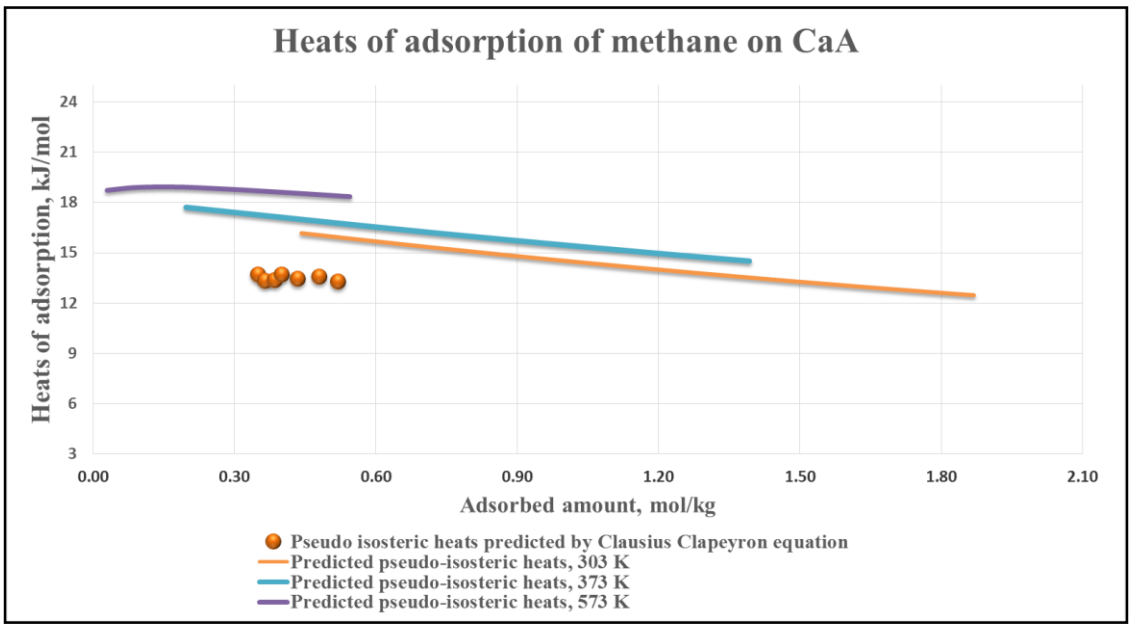

Figure 25: Comparison of model-predicted isosteric heats of adsorption for methane-CaA system with the Clausius-Clapeyron equation results

Figure 25 also reflects the decrease of isosteric heats of adsorption with loading at the three temperatures. A related work on the adsorption of methane and nitrogen on zeolite 5A (CaA), done by Bakhtyari and Mofarahi [43], shows that heats of adsorption of methane on CaA zeolite decrease with adsorbed amount at the low loading region and are constant with adsorbed amount after that. Another related work, by Nam *et al.* [45], shows the opposite, i.e., that the heats of adsorption of methane-CaA system increase with adsorbed amount. Both Bakhtyari and Mofarahi [43] and Nam *et al.* [45] calculated their heats using the Clausius-Clapeyron equation and did not measure them experimentally. The difference in results among model calculations and literature can be referred to the accuracy of calculating the heats using the Clausius-Clapeyron equation and to the type and specific characteristics of the zeolite used.

It is important to highlight that the results of the Clausius-Clapeyron equation involves some human inaccuracy in reading the (T, P) pairs values from the isotherms Figure. The average values of pseudo-isosteric heats of adsorption obtained from the model and the Clausius-Clapeyron equation are 16 kJ/mol and 13.5 kJ/mol respectively with an average deviation of 38% between the two results.

The calculation of the difference in specific heat capacity between the adsorbed and the gas phases was done for this system as results of calculated isosteric heats were available at three different temperatures. Δc_p of this system is around -0.004 kJ/(mol. K) or –0.5R (where R is the universal gas constant, which is equal to 8.314 J/(mol.K)). The negative sign indicates that the adsorbed phase heat capacity of methane on CaA zeolite is less than the bulk phase heat capacity by “0.5R”.

4.3.2. Heats of adsorption of methane-NaX system

For the system of methane – NaX, the isosteric heats of adsorption were predicted as well as the pseudo-isosteric heats using the model at 304.45 K that were compared to calorimetric measurements of pseudo-isosteric heats done by Dunne *et al.* [21] who measured pseudo-isosteric heats of adsorption of different pure gases on NaX zeolite using a Tian-Calvet calorimeter. The results are presented in Figure 26. The predicted isosteric heats, pseudo-isosteric heats, and calorimetric heats have average values of 11.1 kJ/mol, 13.5 kJ/mol and 19.3 kJ/mol respectively. All heats are of the same order of magnitude and follow the common of having almost constant values with increased adsorbed amount, which reflects surface homogeneity of zeolite NaX towards the adsorption of methane molecules. According to Dunne *et al.* [21], this represents a balance between energetic heterogeneity of the gas-solid interactions and the gas-gas interactions. The average difference between the predicted pseudo-isosteric heats and the calorimetric pseudo-isosteric heats is around 6 kJ/mol or 30%.

Calculations of difference in specific heat capacity between the adsorbed and gas phase were not made due to the unavailability of isosteric heats at different temperatures for this system.

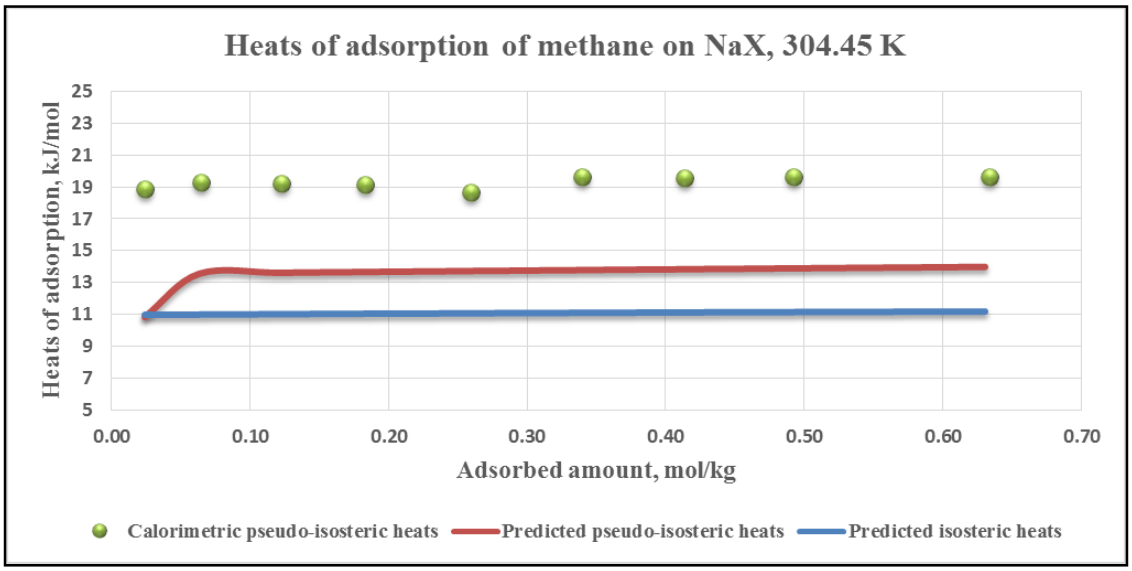

Figure 26: Predicted vs. calorimetric (adapted from [21]) heats of adsorption of methane-NaX system

4.3.3. Heats of adsorption of ethane-CaA system

For this system, the isosteric heats of adsorption as well as the pseudo-isosteric heats were predicted using the model's equation and plotted vs. adsorbed amount for three different temperatures.

Figure 27 shows the decrease in isosteric heats of adsorption of ethane on CaA zeolite with the increased adsorbed amount. This is a sign of the surface heterogeneity of zeolite CaA towards adsorption of ethane molecules. The decrease in model-predicted isosteric heats is in the range of 1.5- 7.5%. The average value of isosteric heats of adsorption of this system is around 15 kJ/mol.

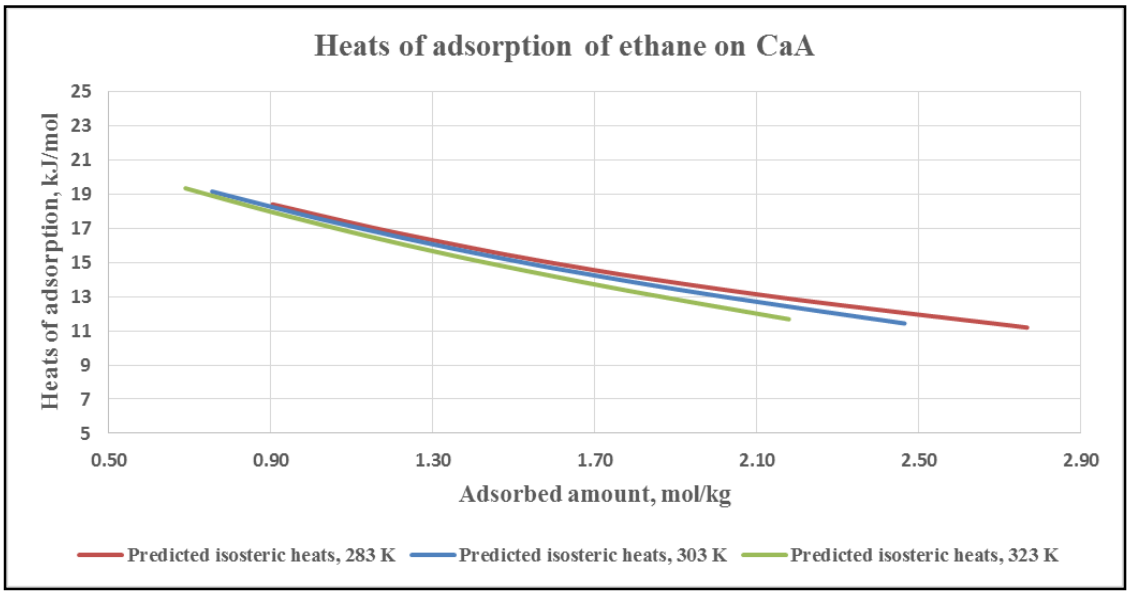

Figure 27: Model-predicted isosteric heats of adsorption for ethane-CaA system

Due to the unavailability of the calorimetric (experimental) measurements of pseudo-isosteric heats of adsorption for this system, the pseudo-isosteric heats were predicted using the Clausius-Clapeyron equation and compared to the model heats. The results of these calculations are expressed in Figure 28. As this figure shows, the pseudo-isosteric heats of adsorption predicted by the model decrease with increased adsorbed amount which disagrees with results obtained from Clausius – Clapeyron equation. Related work on the adsorption of ethane and ethylene on zeolite 5A (CaA) that was done by Mofarahi and Salehi [33] and by Nam *et al.* [45], show that pseudo-isosteric heats of adsorption of ethane on 5A zeolite increase as the adsorbed amount increases in the low loading region and is constant after that. Bakhtyari and Mofarahi [43] and Nam

et al. [45] calculated their pseudo-isosteric heats using the Clausius-Clapeyron equation and did not measure them experimentally.

The average values of the pseudo-isosteric heats of adsorption obtained from the model and the Clausius-Clapeyron equation are around 19 kJ/mol and 25.3 kJ/mol respectively. The average difference between the model results and Clapeyron equation results of pseudo-isosteric heats is around 46%. The main reason behind this difference is the difference between the predicted and experimental adsorption isotherms of this system that were discussed in Section 4.2 as well as the error embedded in the graphical reading for the Clausius-Clapeyron equation calculations.

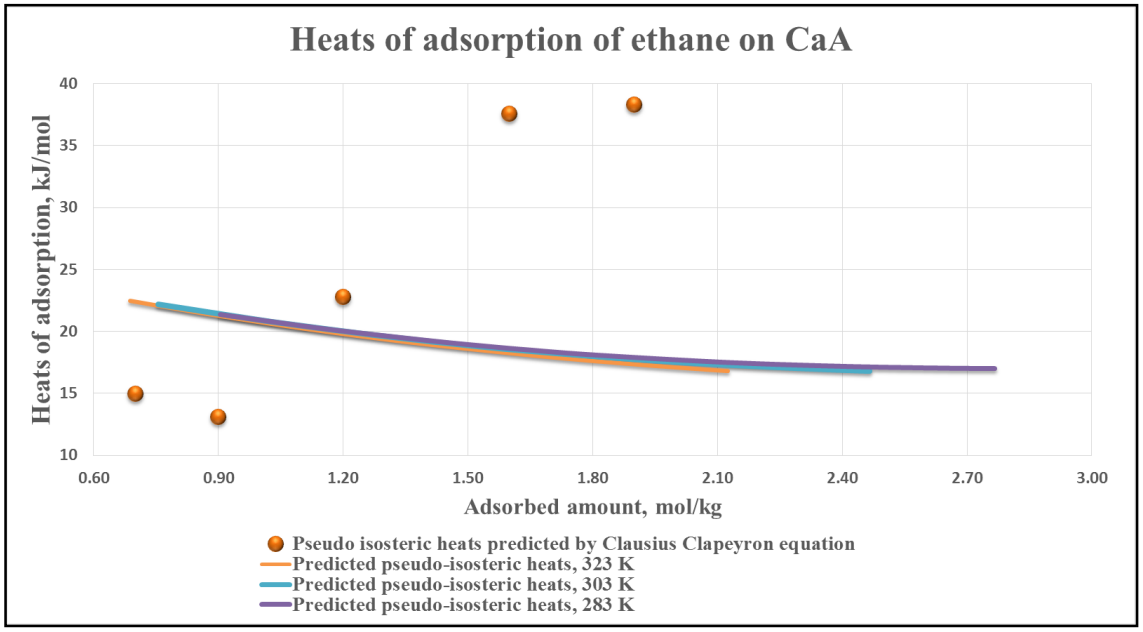

Figure 28: Comparison of model-predicted isosteric heats of adsorption for ethane-CaA system with the Clausius-Clapeyron equation results

The calculation of the difference in specific heat capacity between the adsorbed and the gas phases was done for this system as results of calculated isosteric heats were available at three different temperatures. Δc_p of this system is around 0.018 kJ/mol. K or 2R. The positive sign indicates that the adsorbed phase heat capacity of ethane on CaA is greater than the gas phase heat capacity by "2R".

4.3.4. Heats of adsorption of ethane-NaX system

For this system of ethane – NaX, the isosteric heats of adsorption as well as the pseudo-isosteric heats were predicted using the model at 305.55 K and compared to calorimetric measurements of pseudo-isosteric heats of adsorption done by Dunne *et al.* [21]. Figure 29 shows the results of the model with comparison to calorimetric measurements of the pseudo-isosteric heats. The predicted isosteric heats, predicted pseudo-isosteric heats, and calorimetric pseudo-isosteric heats have average values of 18.6 kJ/mol, 23.3 kJ/mol, and 30 kJ/mol respectively. Both of the predicted and calorimetric isosteric heats of adsorption have almost the same trend and the same order of magnitude. The predicted isosteric and pseudo-isosteric heats initially increase with adsorbed amount and they are slightly fluctuating at high loading values. The calorimetric heats fluctuate at low loading then gradually increase. The overall increase in the heats of adsorption of this system is around 9% for predicted isosteric heats, 26% for predicted pseudo-isosteric heats, and 21% for calorimetric pseudo-isosteric heats of adsorption.

The above analysis reflects that the surface of the zeolite is of non-heterogeneous type and that the interactions between adsorbed molecules cannot be ignored as it has its effect on isosteric heats of adsorption. This increase basically reflects that the gas-solid interactions are constant and the molecule-molecule interactions are larger as discussed by Dunne *et al.* [21]. The average difference between predicted and calorimetric pseudo-isosteric heats is around 7 kJ/mol or 23%.

Calculations of difference in specific heat capacity between the adsorbed and gas phase were not made due to the unavailability of isosteric heats at different temperatures for this system.

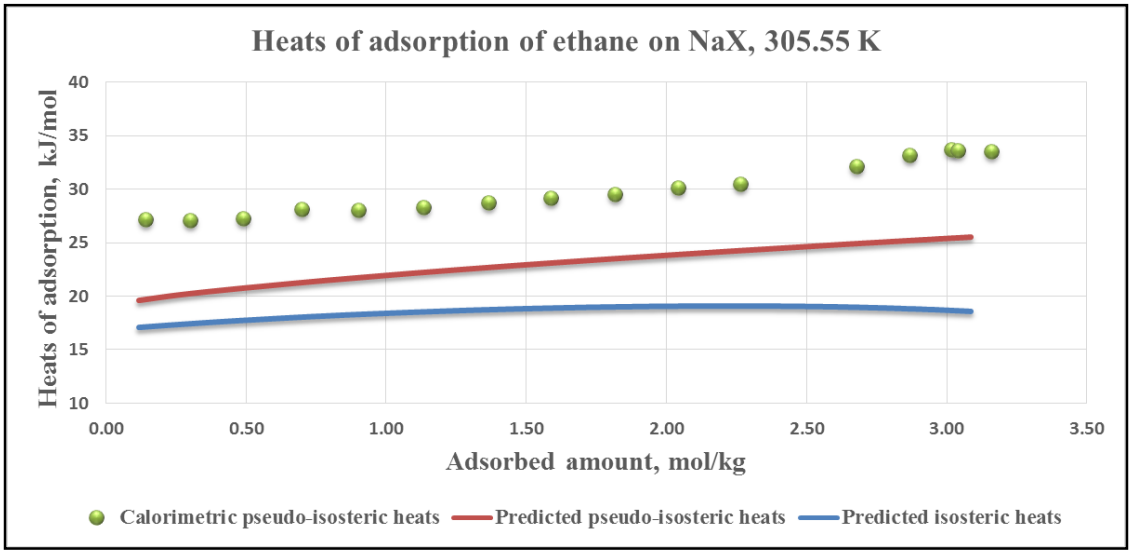

Figure 29: Predicted vs. calorimetric (adapted from [21]) heats of adsorption of ethane-NaX system

4.3.5. Heats of adsorption of nitrogen-CaA system

For the system of nitrogen adsorption on CaA zeolite, the isosteric of adsorption were predicted using the model equation and presented in Figures 30. As shown from this figure, the isosteric heats of adsorption of nitrogen-CaA system are decreasing with increased adsorbed amount, with an overall decrease of 7 – 12%. This reflects the surface heterogeneity of zeolite CaA towards the adsorption of nitrogen molecules. The average values of isosteric heats of adsorption obtained from the model for this system is around 12.3 kJ/mol.

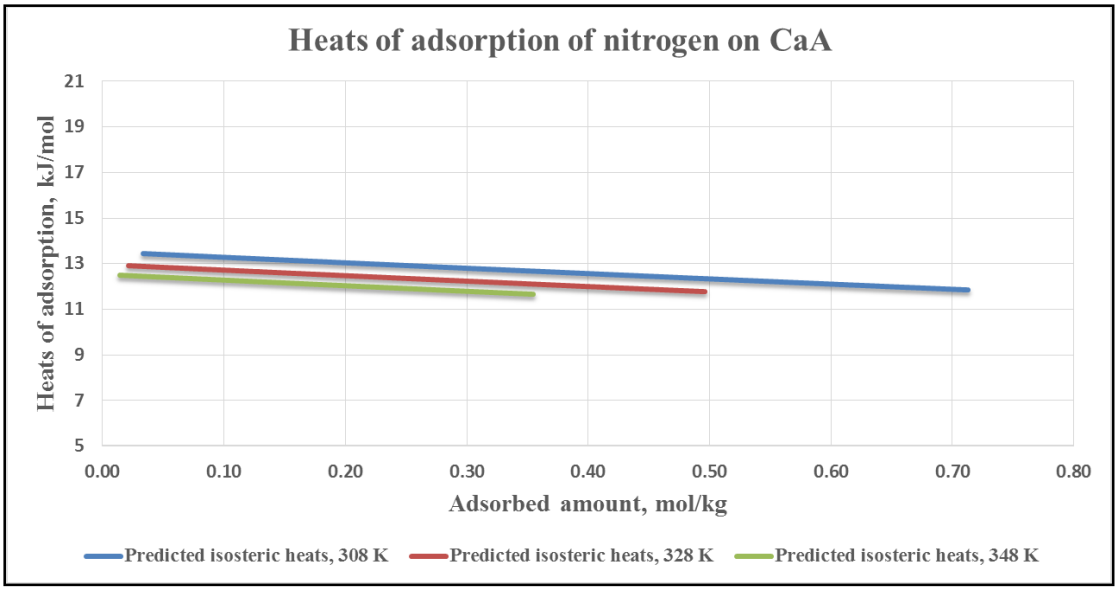

Figure 30: Model-predicted isosteric heats of adsorption for nitrogen-CaA system

The pseudo-isosteric heats of adsorption of this system were also predicted using the Clausius-Clapeyron equation. The results were compared to the predicted isosteric heats of adsorption from the model and presented in Figure 31. Results were also compared to the pseudo-isosteric heats from the Clausius-Clapeyron calculation which were obtained by Shen *et al.*[20]. The average values of pseudo-isosteric heats predicted by the model and Clausius Clapeyron equation are around 15 kJ/mol and 24.5 kJ/mol respectively with an average relative difference of 38%.

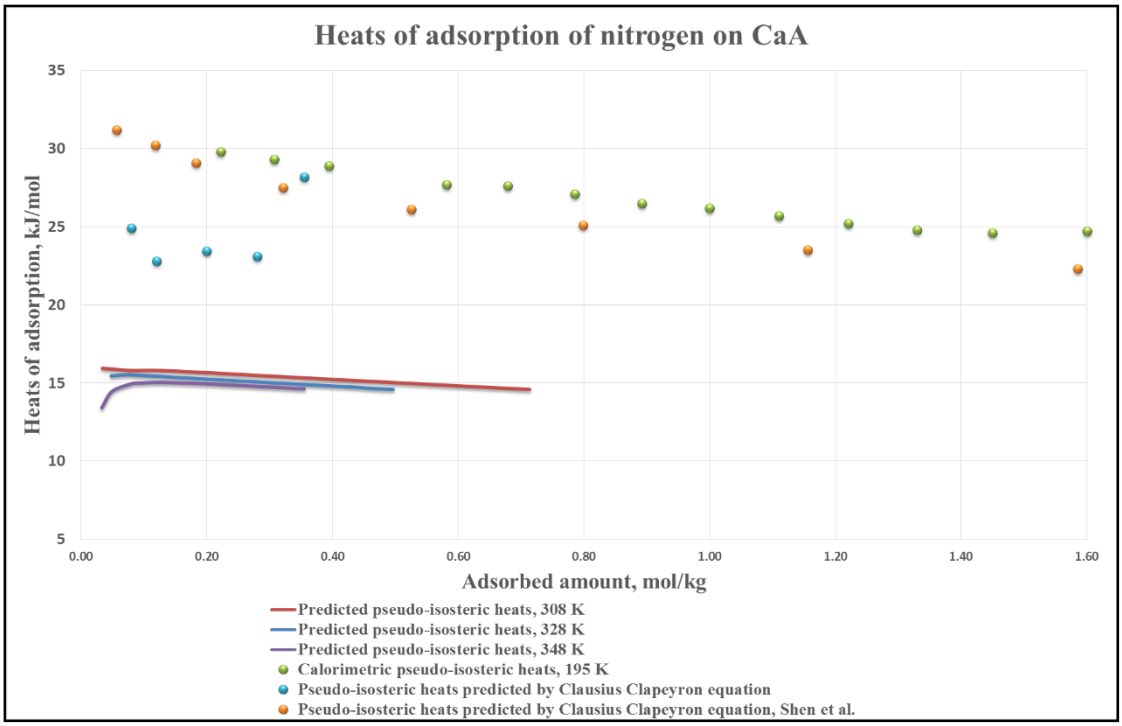

Figure 31: Comparison of model-predicted pseudo-isosteric heats of adsorption for nitrogen-CaA system with the calorimetric and Clausius-Clapeyron equation results. Calorimetric values and Clausius-Clapeyron results of Shen et al. are adapted from [20]

As it can be noticed from Figure 31, the values of predicted pseudo-isosteric heats by Shen *et al.* [20] is in very good agreement with the calorimetric pseudo-isosteric heats reported by them as well. These two are larger than the Clausius-Clapeyron calculations done in this research. The reason behind this is that Shen et al. [20] used the technique of measuring adsorption isosteres described earlier in chapter II instead of estimating these isosteres from adsorption isotherms as done in this research. The use of measured adsorption isosteres is more accurate as they are in much better agreement with experimentally measured heats.

Shen *et al.* [20] also provided calorimetric measurements of isosteric heats of adsorption of nitrogen on CaA zeolite, however, they were measured at 195 K which differs from the temperature range used in the model calculations (308 – 348 K). Since there is a difference in temperature, model results cannot be compared to these experimental measurements.

The calculation of the difference in specific heat capacity between the adsorbed and the gas phases was done for this system as results of calculated isosteric heats were available at three different temperatures. Δc_p of this system is around 0.025 kJ/mol. K or 3R. The positive sign indicates that the adsorbed phase heat capacity of Nitrogen on CaA is greater than the gas phase heat capacity by "3R". As these results indicate that isosteric heats of this system change with temperature, a comparison between the calculated heats at 308 K and the measured heats at 195 K was made to compare the trend and behavior only and not the values. Figure 31 shows the results of this comparison and clearly highlights the previous findings of the decreasing isosteric heats

of adsorption of this system with increased adsorbed amount. This agrees with the results found by Shen *et al.*[20].

4.3.6. Heats of adsorption of nitrogen-NaX system

The isosteric and pseudo-isosteric heats of adsorption of nitrogen – NaX zeolite were predicted using this model's equation at 305.65 K. The predicted pseudo-isosteric heats were compared to the calorimeter measurements done by Dunne *et al.* [21] at the same temperature. The results of the predictions are presented in Figure 32. The predicted isosteric, predicted pseudo-isosteric, and calorimetric pseudo-isosteric heats have average values of 9.6 kJ/mol, 12 kJ/mol, and 19.1 kJ/mol respectively. All of the heats of adsorption of this system have almost the same trend and behavior as well as the same order of magnitude. The predicted isosteric heats of adsorption is constant with increased adsorbed amount and the pseudo-isosteric heats of adsorption has also the same behavior despite the increase in heats for adsorbed amounts less than 0.05 mol/kg. The calorimetric pseudo-isosteric heats fluctuate by an average of 1.8% between each two points but its general trend is constant with adsorbed amount as well. The model-predicted heats of this system show that NaX is a homogenous adsorbent for nitrogen molecules, however, the calorimetric measurements reflect that NaX zeolite is energetically heterogeneous towards nitrogen molecules and that the interactions between adsorbed molecules cannot be ignored as it has its effect on the heats of adsorption. The average difference between the predicted and calorimetric pseudo-isosteric heats is around 7.2 kJ/mol or 35%.

Calculations of difference in specific heat capacity between the adsorbed and gas phase were not made due to the unavailability of isosteric heats at different temperatures for this system.

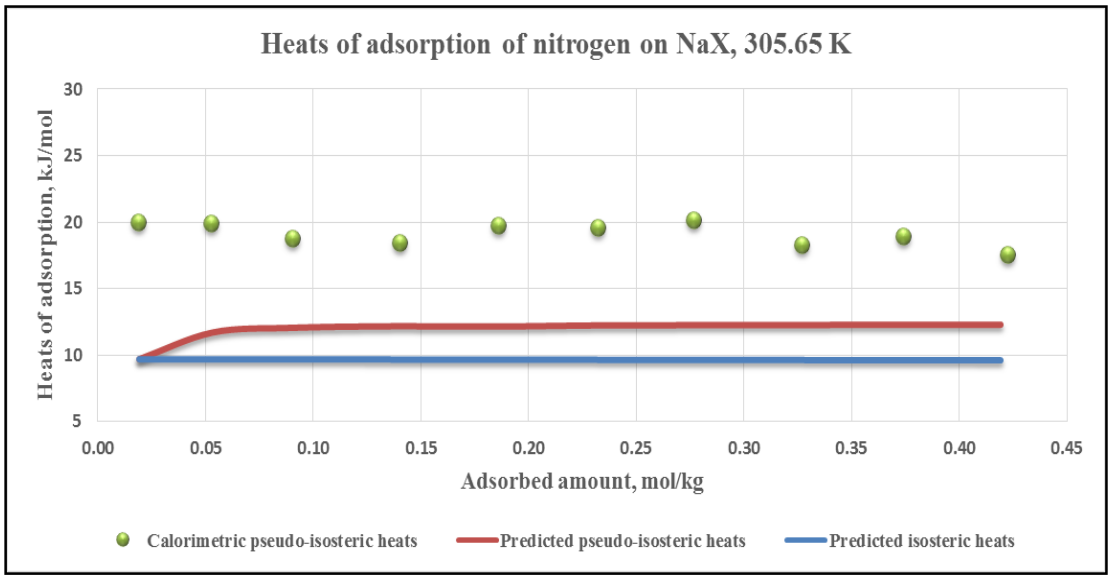

Figure 32: Predicted vs. calorimetric (adapted from [21]) heats of adsorption of nitrogen-NaX system

4.3.7. Heats of adsorption of oxygen-CaA system

For the system of oxygen adsorption on CaA zeolite the isosteric heats of adsorption were predicted using the model equation and presented in Figure 33. As this figure shows, the isosteric heats of adsorption of oxygen-CaA system are slightly decreasing with increased adsorbed amount with an overall decrease of 4% only. This

shows that there are some energetic heterogeneity interactions between the oxygen molecules and CaA zeolite.

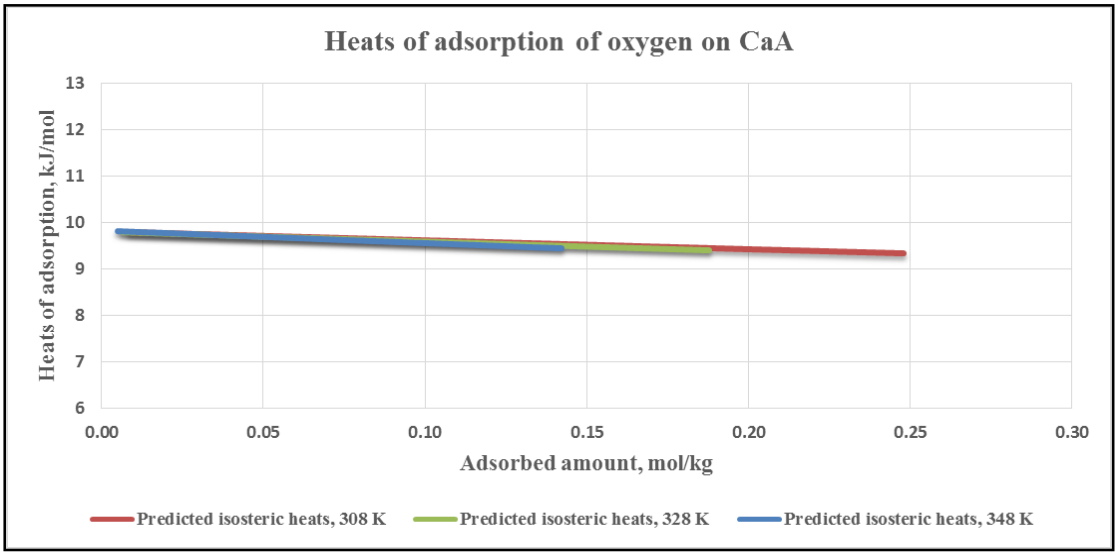

Figure 33: Model-predicted isosteric heats of adsorption for oxygen-CaA system

The pseudo-isosteric heats of adsorption of this system were also predicted using the model and compared with the results from Clausius Clapeyron equation as well as calorimetric measurements of pseudo-isosteric heats measured at 195 K. Figure 34 shows the results of these calculations and compares them with Clausius Clapeyron results found by Shen *et al.* [20]. As this figure shows, the pseudo-isosteric heats predicted by the model increase up to a loading value of 0.02 mol/kg and then stay almost constant with increased adsorbed amount. The calorimetric heats and Clausius Clapyeron heats have a fluctuating behavior with increased adsorbed amount.

The predicted isosteric heats have an average value of 9.6 kJ/mol. The pseudo-isosteric heats predicted by the model, Clausius Clapeyron, and measured experimentally have average values of 10.8 kJ/mol, 15 kJ/mol, and 17.8 kJ/mol respectively. The average relative difference between model-predicted and Clausius Clapeyron pseudo-isosteric heats is around 21%. Shen *et al.* [20] also provided calorimetric measurements of isosteric heats of adsorption of oxygen on CaA zeolite, however, they were measured at 195 K which differs from the temperature range used in the model calculations (308 – 348 K). Since there is a difference in temperature, model results cannot be compared to these experimental measurements.

The calculation of the difference in specific heat capacity between the adsorbed and the gas phases was done for the oxygen – CaA system as results of predicted isosteric heats were available at three different temperatures. Δc_p of this system is around 0.0012 kJ/mol. K or 0.15R. The positive sign indicates that the adsorbed phase heat capacity of oxygen on CaA is greater than the gas phase heat capacity by "0.15R". As these results point out that isosteric heats of this system change with temperature, a comparison between the calculated heats at 308 K and the measured heats at 195 K was made to compare the trend and behavior only and not the values.

The results of this system show that CaA zeolite is somehow energetically heterogeneous towards oxygen molecules and that the interactions between the adsorbate molecules exist and cannot be ignored.

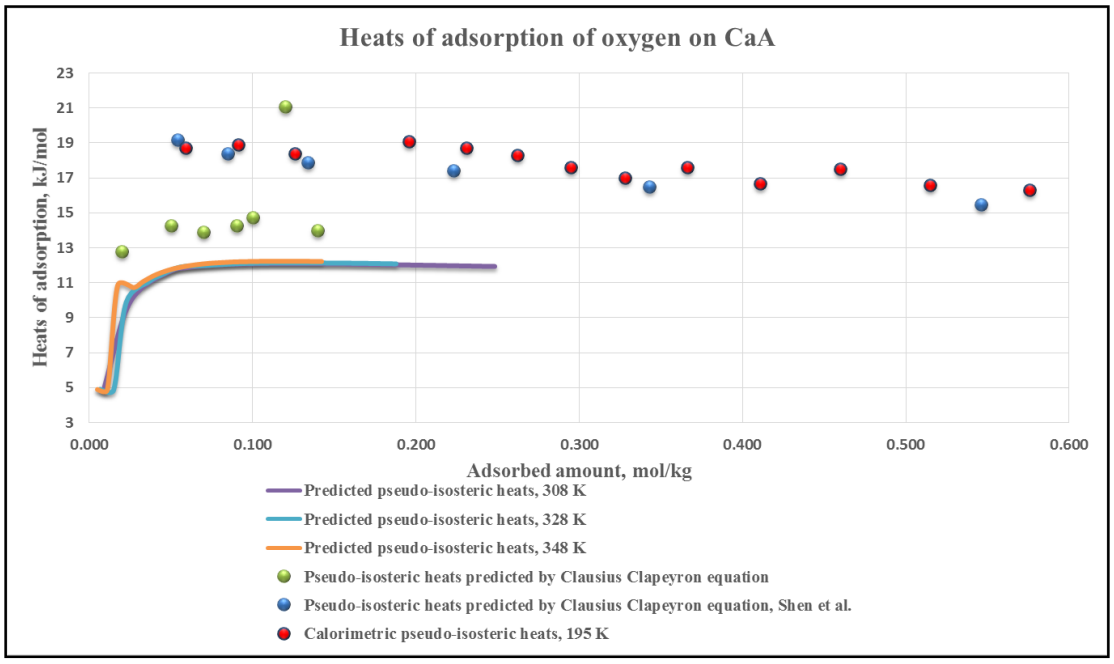

Figure 34: Comparison of model-predicted pseudo-isosteric heats of adsorption for oxygen-CaA system with the calorimetric and Clausius-Clapeyron equation results. Calorimetric values and Clausius-Clapeyron results of Shen et al. are adapted from [20]

4.3.8. Heats of adsorption of oxygen-NaX system

The isosteric and pseudo-isosteric heats of adsorption were predicted at 306.35 K for the system of oxygen – NaX. Comparison with calorimetric measurements of pseudo-isosteric heats were made at the same temperature using the experimentally measured heats of adsorption by Dunne *et al.* [21]. The results of the calculations and the comparison with calorimetric heats are presented in Figure 35.

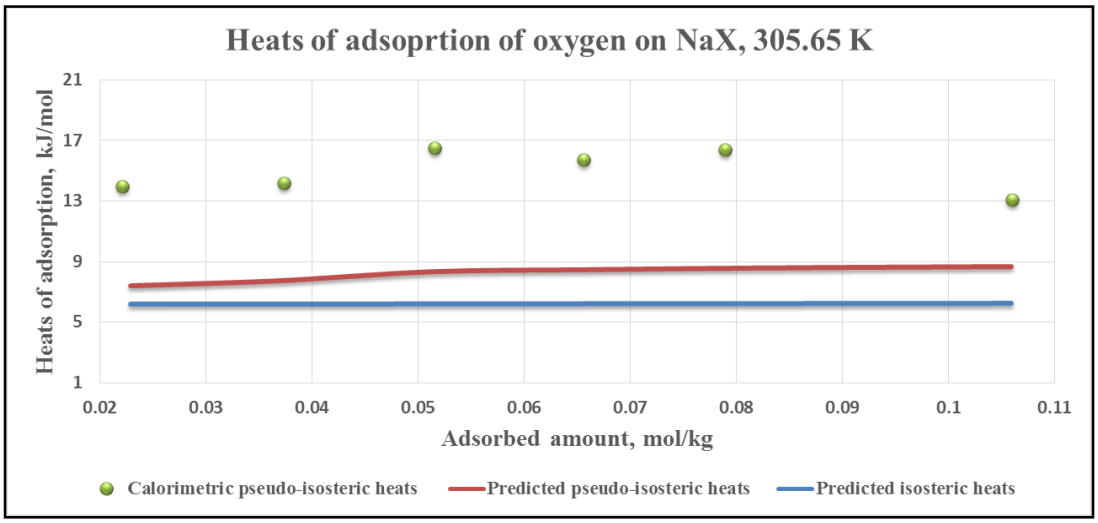

Figure 35: Predicted vs. calorimetric (adapted from [21]) heats of adsorption of oxygen-NaX system

As shown in Figure 35, the predicted isosteric, predicted pseudo-isosteric, and calorimetric pseudo-isosteric heats have average isosteric heats of adsorption of 6.2 kJ/mol, 8.3 kJ/mol, and 14.9 kJ/mol respectively. The predicted heats are almost constant with the increased adsorbed amount. The calorimetric heats of adsorption fluctuate with an overall change of around 2.4%. This fluctuation in calorimetric heats can be attributed to the accuracy in experimental procedure done as well as to the different levels of energetic heterogeneity of zeolite NaX towards oxygen molecules. The average relative difference between predicted and calorimetric pseudo-isosteric heats is around 6.8 kJ/mol or 45%.

Calculations of difference in specific heat capacity between the adsorbed and gas phase were not made due to the unavailability of isosteric heats at different temperatures for this system.

4.3.9. Heats of adsorption of argon-NaX system

The isosteric and pseudo-isosteric heats of adsorption of the argon – NaX system were predicted using the models' equation at 304.15 K. The results were compared to experimentally measured pseudo-isosteric heats from the work done by Dunne *et al.* [21]. The results with comparison are presented in Figure 36. As this figure shows, the predicted isosteric heats are constant with increased adsorbed amount. The predicted pseudo-isosteric heats, however, experience an increase up to a loading value of 0.023 mol/kg and then become constant with increased adsorbed amount. The calorimetric pseudo-isosteric heats fluctuate, but are somehow constant with increased adsorbed amount. The predicted isosteric, predicted pseudo-isosteric, and calorimetric pseudo-isosteric heats have average values of 7.2 kJ/mol, 8.6 kJ/mol, and 12.7 kJ/mol respectively. The obtained results of this system reflect the surface homogeneity of zeolite NaX towards argon molecules. The predicted and calorimetric pseudo-isosteric heats have a difference of 4.2 kJ/mol or 33%.

Calculations of difference in specific heat capacity between the adsorbed and gas phase were not made due to the unavailability of isosteric heats at different temperatures for this system.

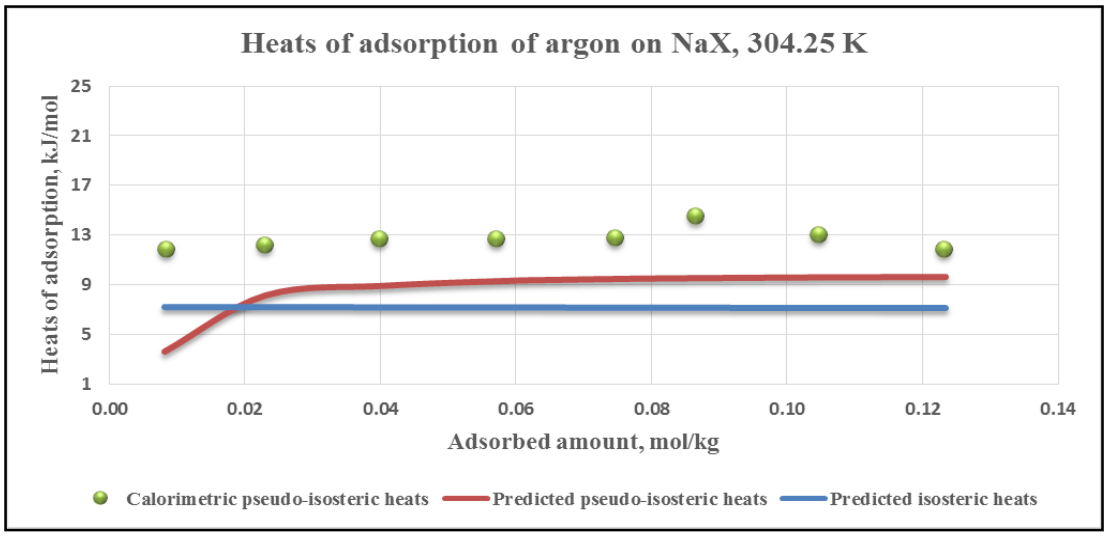

Figure 36: Predicted vs. calorimetric (adapted from [21]) heats of adsorption of argon-NaX system

4.3.10. Heats of adsorption of carbon dioxide-NaX system

The isosteric and pseudo-isosteric heats of adsorption of carbon dioxide on NaX zeolite were predicted using the model's equation at 304.55 K and 305.95 K and presented in Figures 37 and 38. The pseudo-isosteric heats were compared to calorimetric measurements from the work of Dunne *et al.* [21]. As both figures show, the predicted and calorimetric heats of adsorption of CO_2 – NaX system follow the same trend, which is the decrease of heats with increased adsorbed amount. The overall decrease in the heats of this system is on average around 25%. Results are in good agreement and reflect the surface heterogeneity of zeolite NaX towards carbon dioxide molecules. The decrease in heats of adsorption for this system is higher at the low

loading region and becomes smaller at higher loading value due to the saturation of adsorption sites and the decrease in energetic interactions between CO_2 and the zeolite.

The predicted isosteric, predicted pseudo-isosteric, and calorimetric pseudo-isosteric heats of adsorption have average values of (25.7 kJ/mol, 30.1 kJ/mol, and 39.3 kJ/mol) at 305.95 K and (24.7 kJ/mol, 30.1 kJ/mol, and 38.3 kJ/mol) at 304.55 K respectively. These findings are in good agreement with the work done by Dunne *et al.* [21] who discussed the decrease in heats of adsorption of CO_2 on NaX zeolite and attributed this decrease to the sensitivity of CO_2 molecules towards the electric filed that exists inside the zeolite and the interactions of the Na^+ ion in the zeolite with the quadrupole moment of CO_2 molecules [21]. The predicted and calorimetric pseudo-isosteric heats have average difference of 8.8 kJ/mol or 22%.

The calculations of the change in specific heat capacity between the adsorbed phase and the gas phase of this system were not done due to the few points available of equal adsorbed amount in both temperatures data as well as the closeness of the two temperature plots which makes it difficult to obtain accurate readings graphically for pairs of isosteric heats and temperature at the same adsorbed amount.

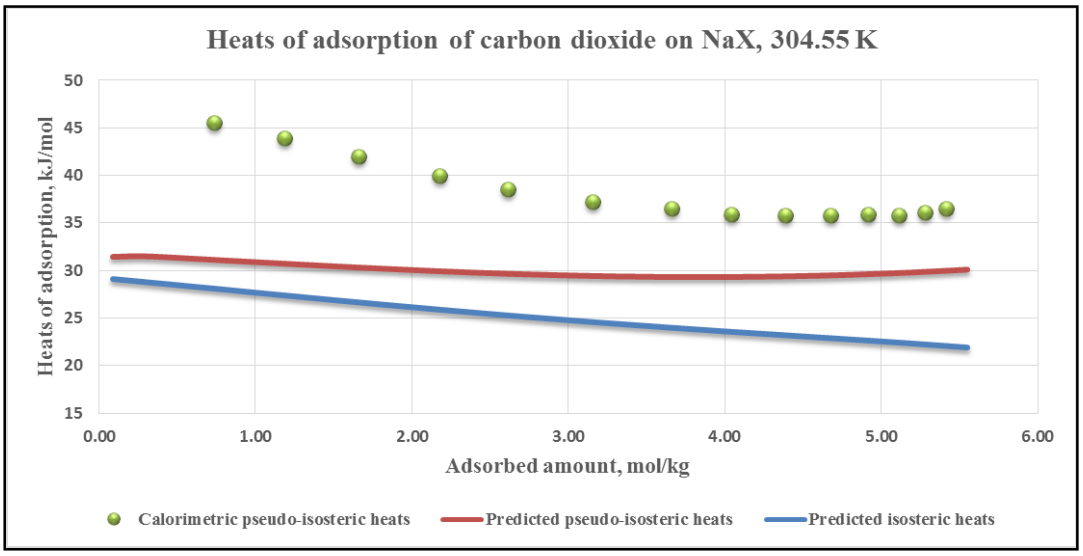

Figure 37: Predicted vs. calorimetric (adapted from [21]) heats of adsorption of carbon dioxide-NaX system at 304.55 K

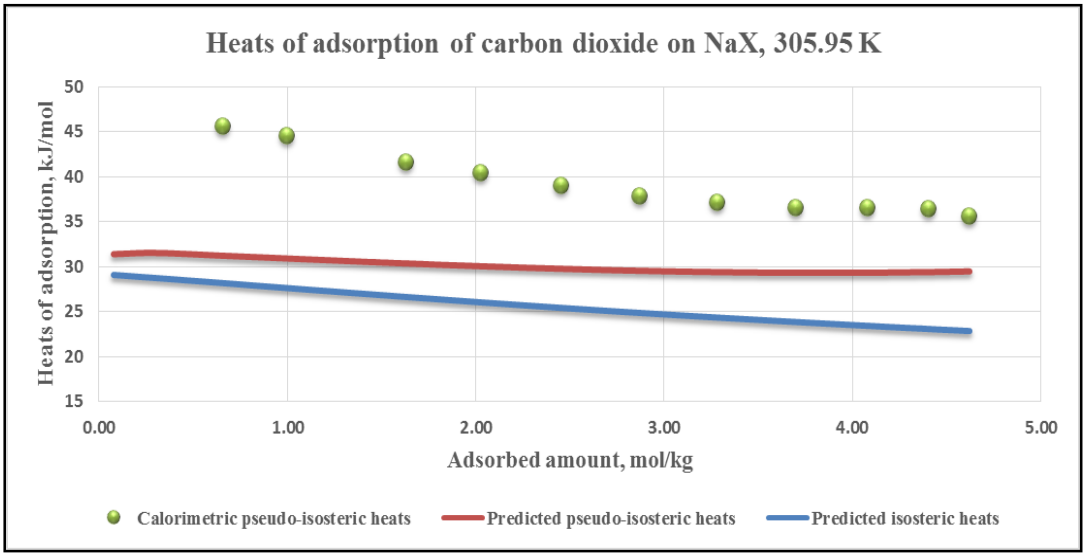

Figure 38: Predicted vs. calorimetric (adapted from [21]) heats of adsorption of carbon dioxide-NaX system at 305.95 K

A summary of the obtained results of isosteric heats of adsorption for the ten systems inspected in this work is available in Table 15. For the adsorption of pure gases on zeolite CaA, ethane has the highest released heats of adsorption, followed by methane and nitrogen, and then oxygen. For the adsorption of pure gases on zeolite NaX, carbon dioxide has the highest released heats of adsorption, followed by ethane, methane, nitrogen, argon, and then oxygen. Components such as methane, nitrogen, and oxygen release higher heats of adsorption on CaA zeolite than that on NaX zeolite. The results of calculations of Δc_p showed that it is in the range of -0.5R to 3R for the adsorption of pure gases on CaA zeolite. There were no available calorimetric Δc_p values in literature for similar systems to compare with, however, some published work on the adsorption of pure gases on zeolites and activated carbon showed that they are in the same order of magnitude. Shen *et al.*[20] found by calculations at two temperature points that Δc_p for oxygen-CaA system is 3R and that Δc_p for nitrogen-CaA system is 5R for the temperature range 195 – 328 K. Walton and LeVan [24] discussed in their work on the adsorbed phase heat capacity that they can change hugely depending on the type of model used to calculate the adsorption isotherms. They discussed that for the case of ideal gas behavior Δc_p is zero if isotherms are calculated using Langmuir equation and that Δc_p is -0.5R if the kinetic theory is used [24].

Table 15: Summary of the predictions of isosteric heats of adsorption

System		*Predicted isos. heats, kJ/mol*	*Predicted pseudo-isos.heats, kJ/mol*	*Clausius Clapeyron heats, kJ/mol*	*Calorimetric heats, kJ/mol*	Δc_p	*Temperature, K*
CaA	Methane	12	16	13.5	-	-0.5R	303
	Ethane	15	19	25	-	2R	303
	Nitrogen	12.3	15	24.5	-	3R	308
	Oxygen	9.6	10.8	15	-	0.15R	308
NaX	Methane	11.1	13.5	-	19.3	-	304.45
	Ethane	18.6	23.3	-	30	-	305.55
	Nitrogen	9.6	12	-	19.14	-	305.65
	Oxygen	6.2	8.3	-	14.96	-	305.65
	Argon	7.2	8.6	-	12.7	-	304.15
	Carbon dioxide	25.7	30.1	-	38.3	-	304.55
	Carbon dioxide	24.7	30.1	-	39.3	-	305.95

The results of the pseudo-isosteric heats of the ten systems presented in this work were compared to calorimetric and/or Clausius Clapeyron equation results since both have the same basis, which is the $RT^2\left(\frac{\partial ln\ P^b}{\partial T}\right)_{v^a}$ term. Tezel *et al.* [46] reported values of heats of adsorption without explaining how they were calculated or at which temperatures they were obtained for three systems that match with this research. The reported heats of adsorption of methane – CaA is 4.45 kcal/mol or 18.6 kJ/mol. For the methane – NaX system, the reported heat are 3.77 kcal/mol or 15.8 kJ/mol. Also, for the ethane – CaA system, the reported heats of adsorption is 6.78 kcal/mol or 28.4 kJ/mol. Comparing these results to the ones found in Table 15, they are closer to the pseudo-isosteric heats of adsorption, with the same order of magnitude.

CHAPTER V

CONCLUSION

The prediction of adsorption isotherms and calorimetric properties of the adsorption process such as the heats of adsorption and adsorbed phase specific heat capacity is of great importance to the design of adsorption – separation processes as they affect their mass and energy balances.

The use of an existing model that extends the Peng Robinson equation of state for fluids confined in spherical adsorbent pores was done in order to predict the adsorption isotherms of pure gases on two different types of zeolites (CaA and NaX). The equation of state used assumes that the interactions between the molecules of the fluid and the pore wall follow the square-well potential and that it can be used for the bulk and confined phases which decreases the level of complexity of calculations.

The use of experimental data available from different reference in a tabular form is absolutely important for the first step of calculations which is the parameter fitting of adsorption isotherms. The fitted parameters are the energy and size parameters. Results of this step showed that the model can correlate adsorption isotherms with a %ARD of 0.4% - 6% for most of the systems except for ethane-CaA system which has a %ARD of around 16%. The model's correlations did not reach the saturation conditions for the systems that reached saturation experimentally as this model predicts saturation at much higher pressure conditions. The reason behind this can be attributed to the cubic equation of state, as usually cubic equations of state do not predict liquid densities accurately.

This affects the results of obtained molar volumes and hence the predicted adsorbed amounts at high pressures. The correlated isotherms and their types are in good agreement with work done by other researchers as was highlighted in chapter IV. The affinity of the same gas on different types of zeolite is very important to determine, as it affects the zeolite selection decision in separation processes.

The fitted isotherms were used for the predictions of the calorimetric properties of adsorption process. The model uses the residual properties in the bulk and confined phases to predict the isosteric and pseudo-isosteric heats of adsorption. The results of predicted pseudo-isosteric heats that were compared to the ones predicted from the Clausius–Clapeyron equation, have a relative difference of 21% - 46%. One of the possible reasons for the large deviation can be the inaccuracy in plots reading for the calculations of the Clausius-Clapeyron equation.

The results of predicted pseudo-isosteric that were compared to calorimetric measurements showed a percentage of relative difference of around 22% - 45%. There are different reasons behind this large deviation between the predicted and measured heats. From the model's point of view, it assumes the same size of all pores in the zeolite and ignores the effect of the cylindrical channels that connect the spherical pores inside the zeolite. A well-structured pore size distribution could produce more accurate results. From calorimetric results point of view, the measured and reported heats of adsorption could be not exactly the isosteric heats of adsorption as there is no agreement on one definition of isosteric heats of adsorption in literature. Although the calorimeter can be designed to measure isosteric heats of adsorption; the measurement of such type of heats

is difficult to obtain with high accuracy as it requires to keep the whole system under constant temperature, which is difficult to maintain, as during the release of heat in adsorption, the temperature changes even if there is a temperature control system inside the calorimeter. Any change in temperature – even if small – affects the type of the collected heats of adsorption and their profile. Despite the difference between the predicted, the calorimeter, and the Clausius-Clapeyron isosteric heats of adsorption, the obtained heats profiles are of the same order of magnitude and trend and reflect on the surface heterogeneity of the zeolite towards the pure gas molecules.

Isosteric heats of adsorption that were obtained at three different temperatures were used to calculate the difference in specific heat capacity between the adsorbed and the bulk gas phases. The obtained results are in the same order of magnitude of results found in literature for different systems. The adsorbed phase heat capacity is very critical to the energy balance in the adsorption column as it is related to the sensible heat released in the column. If this specific heat is not calculated properly, it deviates the energy balance from the accurate values.

The EOS used in this research has shown to be reliable because of its capability in correlating adsorption isotherms with small average relative difference percentages. The calculated difference in specific heat capacity is another indication of the reliability of the model because the found values are within the range of published data. Another way to assess the reliability of the model is to calculate Henry's constant at the low pressure region of the adsorption isotherm and compare it with published constants found using other reliable models.

This work can be further developed to enhance the quality of the results obtained from it. The way it is structured is very efficient in terms of correlating adsorption isotherms, predicting isosteric heats of adsorption, and adsorbed phase heat capacity which – if used properly – can help with the material and energy balances of adsorption columns which affects their preliminary design, size, utility requirement, and cost.

CHAPTER VI

FUTURE WORK

The model that is used in this work can be considered as the basis for many types of applications and areas of improvement for adsorption related calculations. It has been used in this thesis to correlate adsorption isotherms, predict isosteric heats of adsorption, and calculate difference in specific heat capacity for pure gas components in spherical pore zeolites of equal pore size.

Future work with this model can use it to do analogous calculations for mixtures of gases as they are of great interest to the gas separation and purifications industry. It can also be tested for its capability to estimate adsorption isotherms and heats of adsorption for liquids on different types of adsorbents.

The model can be further developed to account for different pore sizes geometry by implementing the pore size distribution in the calculations. This should enhance the quality and accuracy of the produced results and will make them closer to experimental measurements. Development of the model to account for the different types of cations available on the zeolite is another area to consider, as it will enhance the accuracy of the obtained results by assuring that the properties of the zeolite used in the calculations is as close as possible to the real zeolite used for the experiments. The significance of this lies in the effect of the cation type available on the surface of the zeolite, on the gas–solid interactions which affects the fitted adsorption isotherms, heats of adsorption, and adsorbed phase heat capacity.

Although ten systems have been studied in this work, it will always be good to test it for different types of gases and adsorbents combinations to check its capability of predictions for a larger variety of adsorbate–adsorbents systems.

As the model overestimates saturation conditions as was shown in chapter IV, it is of great interest to investigate the reason behind this in order to improve the model's performance in predictions and parameter fitting. This can be done using molecular simulation. Molecular simulation can be carried out with the same assumptions used in this model to diagnose its computational approach as well as its assumptions.

This model was used for zeolites of spherical pores geometry so, another area of application is to use it in the calculations related to zeolites with cylindrical pore geometry such as ZSM-5. Such type of work was done by Barbosa [47] who developed the model for cylindrical pore geometry using molecular simulation. Barbosa [47] evaluated the geometrical and energetic effects of the adsorbent on confined fluids. He assumed a cylindrical box at which the molecules are fluctuating, and modeled them using the hard sphere model [47].

Once verified for its capability in this area, it can be further developed to predict adsorption properties on zeolites of heterogeneous pore size geometry that combines spherical and cylindrical pore structures.

Another potential area for model development is to study how the model can be used to correlate chemisorption isotherms. This requires a thorough study and understanding of the chemisorption phenomena which mainly involves the formation of monolayer and the transfer of electron charges between adsorbate and adsorbent as well

as the chemical reactions that adsorbate molecules undergo on the adsorbent surface and inside its pores. Calculations of chemisorption isotherms involve the determination of the effect that electron transfer interactions have on the extent of the amounts adsorbed in the form of collection amount adsorbed versus bulk pressure. The existing models that are used to correlate/predict physical adsorption cannot be used in the same manner for chemisorption as they do not count for the strong electron transfer interactions induced by chemisorption. Further studies of the structure of the model used in this work will be required to better estimate these interactions and accurately correlate chemisorption isotherms.

The model, as used in this thesis, is a correlative model for adsorption isotherms and a predictive model for heats of adsorption. However, it is possible to envisage several variations of this strategy. One of them is to fit adsorption isotherm and heats of adsorption data simultaneously. The likely outcome of this fully correlative approach will be an improvement in the results for heats of adsorption and some degradation of the results for adsorption isotherms. The opposite approach of turning the model as predictive as possible is more difficult. For conventional phase equilibrium, group contribution methods have achieved remarkable success in predictive calculations. The historical development of these methods relied on large amounts of good-quality experimental vapor-liquid and liquid-liquid equilibrium data. The amount of adsorption equilibrium data available in the literature is much smaller and strongly depends on the characteristics of the solid adsorbent. Data for seemingly the same system from different research groups can be quite different and this poses a challenge to the development of

group-contribution schemes. Molecular simulations may be the path toward an overall predictive approach. Monte Carlo and/or molecular dynamics simulations, now capable of predicting adsorption isotherms with acceptable accuracy for many systems, could be used to generate pseudo-experimental data, which could then be used to fit the EOS parameters. While the EOS calculation itself would still be correlative, the overall approach would be predictive.

REFERENCES

[1] L. Travalloni, M. Castier, F. W. Tavares, and S. I. Sandler, "Critical Behavior of Pure Confined Fluids from an Extension of the van der Waals Equation of State," *J. Supercrit. Fluids*, vol. 55, no. 2, pp. 455–461, 2010.

[2] R. Roque-Malherbe, *Adsorption and Diffusion in Nanoporous Materials*. Boca Raton, FL: CRC Press, 2007.

[3] D. M. Ruthven, *Principles of Adsorption and Adsorption Processes*. New York: John Wiley & Sons Inc., 1984.

[4] J. Seader and E. J. Henley, *Separation Process Principles*, 2nd ed. Hoboken, N.J: John Wiley & Sons, Inc., 2006.

[5] A. Chakraborty, B. B. Saha, I. I. El-Sharkawy, S. Koyama, K. Srinivasan, and K. C. Ng, "Theory and Experimental Validation on Isosteric Heat of Adsorption for an Adsorbent + Adsorbate System," *High Temp. - High Press.*, vol. 37, no. 2, pp. 109–117, 2008.

[6] R. T. Yang, *Gas Separation by Adsorption Processes*. London: Imperial College Press, 1997.

[7] J. Keller and R. Staudt, *Gas Adsorption Equilibria: Experimental Methods and Adsorption Isotherms*. Boston: Springer Science & Business Media, Inc, 2005.

[8] A. L. Myers, "Thermodynamics of Adsorption in Porous Materials," *AIChE J.*, vol. 48, no. 1, pp. 145–160, 2002.

[9] L. Travalloni, M. Castier, F. W. Tavares, and S. I. Sandler, "Thermodynamic Modeling of Confined Fluids Using an Extension of the Generalized van der Waals Theory," *Chem. Eng. Sci.*, vol. 65, no. 10, pp. 3088–3099, 2010.

[10] S. Brunauer, L. S. Deming, W. E. Deming, and E. Teller, "On a Theory of the Van der Waals Adsorption of Gases," *J. Am. Chem. Soc*, vol. 62, no. 7, pp. 1723–1732, 1940.

[11] T. L. Hill, "Statistical Mechanics of Adsorption. V. Thermodynamics and Heat of Adsorption," *The Journal of Chemical Physics*, vol. 17, no. 6. pp. 520–535, 1949.

[12] D. P. Valenzuela and A. L. Myers, *Adsorption Equilibrium Data Handbook*. Englewood Cliffs, N.J.: Prentice-Hall, 1989.

[13] M. L. D. Lima, "Development of a Thermodynamic Model for Fluids Confined in Spherical Pores", M.S. Thesis, Texas A&M University at Qatar, 2014.

[14] K. S. Walton and M. D. Levan, "Development of Energy Balances for Fixed-Bed Adsorption Processes : Thermodynamic Paths , Heat Capacities and Isosteric Heats," *Adsorption*, vol. 11, no. 1, pp. 555–559, 2005.

[15] F. Karavias and A. L. Myers, "Isosteric Heats of Multicomponent Adsorption: Thermodynamics and Computer Simulations," *Longmuir*, vol. 7, no. 12, pp. 3118–3126, 1991.

[16] S. I. Sandler, S. Builes, and R. Xiong, "Isosteric Heats of Gas and Liquid Adsorption," *Langmuir*, vol. 29, no. 33, pp. 10416–10422, 2013.

[17] S. Sircar, R. Mohr, C. Ristic, and M. B. Rao, "Isosteric Heat of Adsorption: Theory and Experiment," *J. Phys. Chem. B*, vol. 103, no. 31, pp. 6539–6546, 1999.

[18] J. A. Dunne, R. Mariwala, M. Rao, S. Sircar, R. J. Gorte, and A. L. Myers, "Calorimetric Heats of Adsorption and Adsorption Isotherms. 1.O2, N2, Ar, CO2, CH4, C2H6, and SF6 on Silicalite," *Langmuir*, vol. 12, no. 24, pp. 5888–5895, 1996.

[19] J. K. Garbacz, G. Rychlicki, and A. P. Terzyk, "A Comparison of Isosteric and Differential Heats of Gas Adsorption on Microporous Active Carbons," *Adsorpt. Sci. Technol.*, vol. 11, no. 1, pp. 15–29, 1994.

[20] D. Shen, M. Bülow, F. Siperstein, M. Engelhard, and A. L. Myers, "Comparison of Experimental Techniques for Measuring Isosteric Heat of Adsorption," *Adsorption*, vol. 6, no. 4, pp. 275–286, 2000.

[21] J. A. Dunne, M. Rao, S. Sircar, R. J. Gorte, and A. L. Myers, "Calorimetric Heats of Adsorption and Adsorption Isotherms . 2. O2, N2, Ar, CO2, CH4, C2H6 , and SF6 on NaX , H-ZSM-5 , and Na-ZSM-5 Zeolites," *Langmuir*, vol. 12, no. 24, pp. 5896–5904, 1996.

[22] D. Parrillo and R. Gorte, "Design Parameters for the Construction and Operation of Heat-Flow Calorimeters," *Thermochim. Acta*, vol. 312, no. 1–2, pp. 125–132, 1998.

[23] B. E. Handy, S. B. Sharma, B. E. Spiewak, and J. a Dumesic, “A Tian-Calvet Heat-Flux Microcalorimeter for Measurement of Differential Heats of Adsorption,” *Meas. Sci. Technol.*, vol. 4, no. 12, pp. 1350–1356, 1993.

[24] K. S. Walton and M. D. LeVan, “Adsorbed-Phase Heat Capacities: Thermodynamically Consistent Values Determined from Temperature-Dependent Equilibrium Models,” *Ind. Eng. Chem. Res.*, vol. 44, no. 1, pp. 178–182, 2005.

[25] S. a Al-Muhtaseb and J. a Ritter, “Roles of Surface Heterogeneity and Lateral Interactions on the Isosteric Heat of Adsorption and Adsorbed Phase Heat Capacity,” *J. Phys. Chem. B*, vol. 103, no. 13, pp. 2467–2479, 1999.

[26] S. a. Al-Muhtaseb and J. a. Ritter, “A Statistical Mechanical Perspective on the Temperature Dependence of the Isosteric Heat of Adsorption and Adsorbed Phase Heat Capacity,” *J. Phys. Chem. B*, vol. 103, no. 38, pp. 8104–8115, 1999.

[27] K. A. Rahman, W. S. Loh, and K. C. Ng, “Heat of Adsorption and Adsorbed Phase Specific Heat Capacity of Methane/Activated Carbon System,” *Procedia Eng.*, vol. 56, pp. 118–125, 2013.

[28] S. a. Al-Muhtaseb, “Personal communication,” Doha, 2015.

[29] R. T. Yang, *Adsorbents: Fundamentals and Applications*. Hoboken, N.J.: Wiley-Interscience, 2003.

[30] W.J.Thomas and B. Crittenden, *Adsorption Technology and Design*. Oxford; Boston: Butterworth-Heinemann, 1998.

[31] A. Ertan, “CO2, N2 and Ar Adsorption on Zeolites. M.S. Thesis,” İzmir Institute of Technology, 2004.

[32] E. L. First and C. A. Floudas, “ZEOMICS: Zeolites and Microporous Structures Characterization,” 2011. [Online]. Available: http://helios.princeton.edu/zeomics/.

[33] M. Mofarahi and S. M. Salehi, “Pure and Binary Adsorption Isotherms of Ethylene and Ethane on Zeolite 5A,” *Adsorption*, vol. 19, no. 1, pp. 101–110, 2013.

[34] L. Travalloni, M. Castier, and F. W. Tavares, “Phase Equilibrium of Fluids Confined in Porous Media from an Extended Peng-Robinson Equation of State,” *Fluid Phase Equilib.*, vol. 362, pp. 335–341, 2014.

[35] M. Castier, "XSEOS: An Open Software for Chemical Engineering Thermodynamics," *Chem. Eng. Educ.*, vol. 42, no. 2, pp. 74 – 81, 2008.

[36] V. Schwamberger and F. P. Schmidt, "Estimating the Heat Capacity of the Adsorbate-Adsorbent System from Adsorption Equilibria Regarding Thermodynamic Consistency," *Ind. Eng. Chem. Res.*, vol. 52, no. 47, pp. 16958–16965, 2013.

[37] S. I. Sandler, *Chemical, Biochemical, and Engineering Thermodynamics*, 4th ed. Hoboken, N.J.: John Wiley & Sons Inc., 2006.

[38] S. Sircar and A. L. Myers, "Gas Separation by Zeolites," in *Handbook of Zeolite Science and Technology*, S. M. AUERBAC, K. A. CARRADO, and P. K. DUTTA, Eds. New York: Marcel Dekker, Inc., 2003.

[39] N. Mehio, S. Dai, and D. E. Jiang, "Quantum Mechanical Basis for Kinetic Diameters of Small Gaseous Molecules," *J. Phys. Chem. A*, vol. 118, no. 6, pp. 1150–1154, 2014.

[40] X. Du and E. Wu, "Porosity of Microporous Zeolites A, X and ZSM-5 Studied by Small Angle X-ray Scattering and Nitrogen Adsorption," *J. Phys. Chem. Solids*, vol. 68, no. 9, pp. 1692–1699, 2007.

[41] S. Pakseresht, M. Kazemeini, and M. Akbarnejad, "Equilibrium Isotherms for CO, CO2, CH4, and C2H4 on the 5A Molecular Sieve by a Simple Volumetric Apparatus," *Sep. Purif. Technol.*, vol. 28, pp. 53–60, 2002.

[42] H. Huang, W. Zhang, D. Liu, B. Liu, G. Chen, and C. Zhong, "Effect of Temperature on Gas Adsorption and Separation in ZIF-8: A Combined Experimental and Molecular Simulation Study," *Chem. Eng. Sci.*, vol. 66, no. 23, pp. 6297–6305, 2011.

[43] A. Bakhtyari and M. Mofarahi, "Pure and Binary Adsorption Equilibria of Methane and Nitrogen on Zeolite 5A," *J. Chem. Eng. Data*, vol. 59, no. 3, pp. 626–639, 2014.

[44] Si. Cavenati, C. A. Grande, and A. E. Rodrigues, "Adsorption Equilibrium of Methane, Carbon Dioxide and Nitrogen on Zeolite 13X at High Pressures," *J. Chem. Eng. Data*, vol. 49, pp. 1095–1101, 2004.

[45] G. Nam, B. Jeong, S. Kang, B. Lee, and D. Choi, "Equilibrium Isotherms of CH4, C2H6, C2H4, N2, and H2 on Zeolite 5A Using a Static Volumetric Method," *J. Chem. Eng. Data*, vol. 50, pp. 72–76, 2005.

[46] R. W. Triebe, F. H. Tezel, and K. C. Khulbe, “Adsorption of methane, ethane and ethylene on molecular sieve zeolites,” *Gas Sep. Purif.*, vol. 10, no. 1, pp. 81–84, 1996.

[47] G. D. Barbosa, “Modeling of Confined Fluids via Molecular Simulation and Equation of State”, M.S. Thesis, School of Chemistry - Rio de Janeiro, 2015.